Insight on [1,3]thiazolo[4,5-*e*]isoindoles as tubulin polymerization inhibitors

Virginia Spanò,[a] Marilia Barreca,[a] Roberta Rocca,[b,c] Roberta Bortolozzi,[d] Ruoli Bai,[e] Anna Carbone,[a1] Maria Valeria Raimondi,[a] Antonio Palumbo Piccionello,[a] Alessandra Montalbano,[a,*] Stefano Alcaro,[c,f] Ernest Hamel,[e] Giampietro Viola,[d,g,*] and Paola Barraja[a]

[a] Dipartimento di Scienze e Tecnologie Biologiche Chimiche e Farmaceutiche (STEBICEF), Università degli Studi di Palermo, Via Archirafi 32, 90123 Palermo (Italy).

[b] Dipartimento di Medicina Sperimentale e Clinica, Università Magna Græcia di Catanzaro, Viale Europa, 88100 Catanzaro, Italy.

[c] Net4Science srl, Academic Spinoff, Università Magna Græcia di Catanzaro, Viale Europa, 88100 Catanzaro, Italy.

[d] Istituto di Ricerca Pediatrica IRP, Fondazione Città della Speranza, Corso Stati Uniti 4, 35127 Padova, Italy.

[e] Molecular Pharmacology Branch, Developmental Therapeutics Program, Division of Cancer Treatment and Diagnosis, Frederick National Laboratory for Cancer Research, National Cancer Institute, National Institutes of Health, Frederick, Maryland 21702, United States.

[f] Dipartimento di Scienze della Salute, Università Magna Græcia di Catanzaro, Viale Europa, 88100 Catanzaro, Italy.

[g] Dipartimento di Salute della Donna e del Bambino, Laboratorio di Oncoematologia, Università di Padova, via Giustiniani 2, 35131 Padova, Italy.

[1] Present address: Dipartimento di Farmacia, Università degli Studi di Genova, Viale Benedetto XV 3, Genova, 16132, Italy

[*]**Corresponding authors**:

Alessandra Montalbano, Dipartimento di Scienze e Tecnologie Biologiche Chimiche e Farmaceutiche (STEBICEF), Università di Palermo, via Archirafi 32, 90123 Palermo, Italy; e-mail: alessandra.montalbano@unipa.it

Giampietro Viola, Istituto di Ricerca Pediatrica IRP, Fondazione Città della Speranza, Corso Stati Uniti 4, 35127 Padova, Italy; Dipartimento di Salute della Donna e del Bambino, Laboratorio di Oncoematologia, Università di Padova, via Giustiniani 2, 35131 Padova, Italy; giampietro.viola.1@unipd.it

Abstract

A series of [1,3]thiazolo[4,5-*e*]isoindoles has been synthesized through a versatile and high yielding multistep sequence. Evaluation of the antiproliferative activity of the new compounds on the full NCI human tumor cell line panel highlighted several compounds that are able to inhibit tumor cell proliferation at micromolar-submicromolar concentrations. The most active derivative **11g** was found to cause cell cycle arrest at the G2/M phase and induce apoptosis in HeLa cells, following the mitochondrial pathway, making it a lead compound for the discovery of new antimitotic drugs.

Keywords: [1,3]thiazolo[4,5-*e*]isoindoles; apoptosis; cell cycle arrest; tubulin polymerization inhibitors.

1. Introduction

Microtubules are an important molecular target in the search for new treatments of cancer [1]. These organelles are involved in different cellular processes, such as cell signaling, secretion and motility, and they play an important role in cell proliferation, since they constitute the mitotic spindle, an essential structure for chromosome segregation during mitosis and meiosis [1–3]. Agents acting on microtubules interfere with their functions and thus can be highly active in the treatment of cancer. Compared to other classes of antitumor drugs, microtubule-binding agents possess great structural diversity and complexity (for example, taxane, vinca and colchicine site agents). Their action leads to either an increase or a reduction of tubulin polymerization. In particular, agents that target the taxane binding site promote microtubule polymerization while vinca and colchicine site agents induce their depolymerization [4,5]. In both cases, by interfering with microtubule dynamics during mitosis, these compounds act as spindle poisons and cause a block of the cell cycle in G2/M with mitotic catastrophe and apoptotic cell death [6].

Especially since the discovery of the potent antitubulin activity of combretastatin A-4 (CA-4) (Chart 1) [7], many new compounds binding to the colchicine site have been synthesized with the aim of discovering new antitubulin agents with increased specificity for cancer cells, reduced neurotoxicity and/or activity against multidrug resistant (MDR) cells. These compounds are generally characterized by simple structures, improved solubility and a wide therapeutic index, as compared with vinca and taxane site agents [8]. CA-4 strongly inhibits tubulin polymerization and the growth of multiple cancer cell lines, including MDR cell lines overexpressing P-glycoprotein (Pgp) [9]. The European Medicines Agency (EMA) and the US Food and Drug Administration (FDA) approved combretastatin A-4 phosphate (CA-4P) (Chart 1), a water-soluble phosphate prodrug of CA-4, also known as fosbretabulin disodium, as an orphan drug for the treatment of anaplastic thyroid cancer and ovarian cancer [9]. Nevertheless, the olefinic *cis*-double bond of CA-4 turned out to be thermodynamically unstable, isomerizing into a *trans*-double bond during storage and metabolism, leading to a reduction of its activity and thus compromising its clinical use [9]. To overcome this change in configuration, the double-bond has been locked into heterocyclic structures, leading to *cis*-restricted configurations [10]. Interesting results were obtained by replacing the double bond with a [1,3]thiazole ring. In particular, trimethoxyphenyl-arylthiazoles of type **1** (Chart 1) and their positional isomers of type **2** (Chart 1) showed potent antiproliferative effects with subnanomolar IC_{50} values against different tumor cell lines, including MDR lines. Both classes of compounds inhibit tubulin polymerization through binding to the colchicine site, in some cases more efficiently than CA-4, inducing cell cycle arrest in the G2/M phase and cell death by apoptosis [11,12].

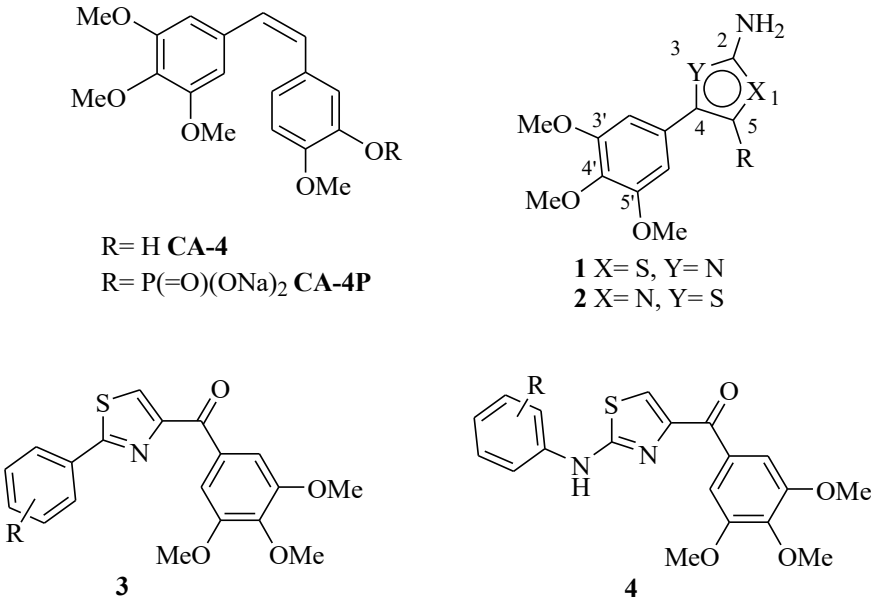

Chart 1. Structures of tubulin polymerization inhibitors.

Similar results were obtained for substituted methoxybenzoyl-arylthiazoles (SMART) of type **3** (Chart 1), which demonstrated a potent *in vitro* antiproliferative effect on the growth of both parental and MDR cell lines and *in vivo* activity. Like the type **1** and type **2** compounds, the SMART compounds disrupt tubulin polymerization by binding to the colchicine site, block the cell cycle in the G2/M phase and cause cell death by apoptosis [13,14]. Chemical optimization of the structure of compounds **3** with the introduction of an amino linkage between the thiazole and the substituted phenyl ring led to phenylamino thiazoles of type **4** (Chart 1), which showed improved solubility and bioavailability compared to the SMART derivatives while preserving strong antiproliferative activity and tubulin polymerization inhibition [15].

Thiazoles are valuable heterocycles in medicinal chemistry, as they are highly represented as the pharmacophore unit of many drug candidates. They show a variety of pharmacological properties, and their analogues offer a high degree of structural diversity as a useful tool for developing new therapeutic agents. Several examples of benzo-fused derivatives, including benzothiazoles (BTA), have been used in clinical practice to treat various diseases with high therapeutic potency, including cancer [16–19].

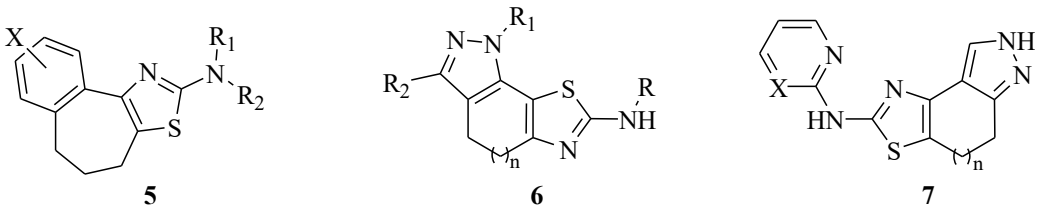

Chart 2. Tricyclic chemical structures containing the thiazole nucleus.

Tricyclic structures incorporating the thiazole nucleus of types **5-7** (Chart 2) were considered for the design of new drug-like molecules [20–22]. For several years, we designed a number of classes of small molecules endowed with biological activity [23–35]. Recently, we reported tricyclic derivatives, [1,2]oxazole[5,4-*e*]isoindoles **8**, [1,2]oxazolo[4,5-*g*]indoles **9** and pyrrolo[2',3':3,4]cyclohepta[1,2-*d*][1,2]oxazoles **10**, as effective tubulin polymerization inhibitors (Chart 3) [36–39]. To further explore the chemical space of our tricyclic structures and, considering that pyrrole condensed systems are characterized by wide structural variability depending on the position occupied by the nitrogen atom, we undertook the synthesis of [1,3]thiazolo[4,5-*e*]isoindol-2-amines of types **11** and **12** (Chart 3) to investigate their biological properties.

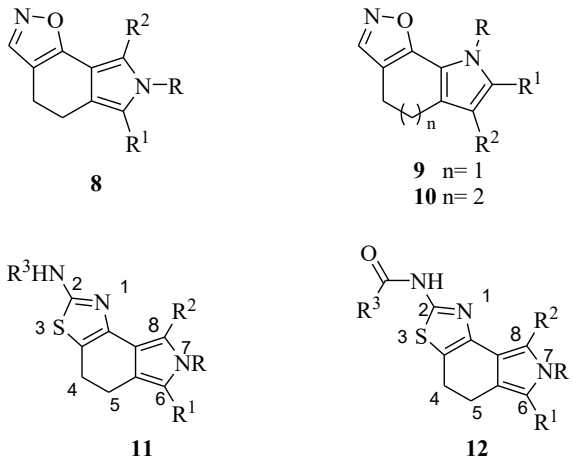

Chart 3 [1,2]oxazolo[5,4-*e*]isoindoles (**8**), [1,2]oxazolo[4,5-*g*]indoles (**9**), pyrrolo[2',3':3,4]cyclohepta[1,2-*d*][1,2]oxazoles (**10**), [1,3]thiazolo[4,5-*e*]isoindol-2-amines (**11**), [1,3]thiazolo[4,5-*e*]isoindol-2-amides (**12**).

2. Results and Discussion

2.1 Chemistry

For the synthesis of the new title ring system, suitable building blocks were the α-bromoketones of type **15**, where the annular carbonyl and the ipso-carbon bearing the bromine atom are two vicinal electrophilic centres, available for further reactions with dinucleophiles. Thus, under typical Hantzsch reaction conditions, they can react with thioureas leading to aminothiazole cyclization. The synthetic strategy to obtain the desired [1,3]thiazolo[4,5-*e*]isoindoles of types **11** and **12** is

outlined in Scheme 1. We started from tetrahydroisoindole-4-ones **13a-c**, which were prepared according to our published procedures [40–42]. Ketones **13a-c** were subjected to nucleophilic reactions with aralkyl halides such as benzenesulfonyl chloride, benzyl bromide or 4-methoxybenzyl chloride in the presence of sodium hydride to give *N*-substituted derivatives **14a-i** in 60−90% yields (Scheme 1). Due to the high reactivity of pyrrole positions, selective bromination of ketones **14** at the position α to the carbonyl group was not successful. In fact, reaction of derivatives **14b,c,e,f,h,i** with an excess of bromine, required to avoid recovery of unreacted starting material or intermediates, brominated only on the pyrrole positions, and a catalytic amount of hydrobromic acid (45% in AcOH) led to tri-brominated products **15b,c** and di-brominated compounds **15e,f,h,i** (45-78%) (Scheme 1). The presence of an electron withdrawing group at the pyrrole nitrogen atom was crucial for direct bromination at the position α to the carbonyl. Thus, ketones **14a,d,g** bearing a phenylsulfonyl group were easily subjected to bromination using pyridine hydrobromide perbromide and led to α-brominated compounds **15a,d,g** in good yield (79-90%) while avoiding other bromination by-products (Scheme 1).

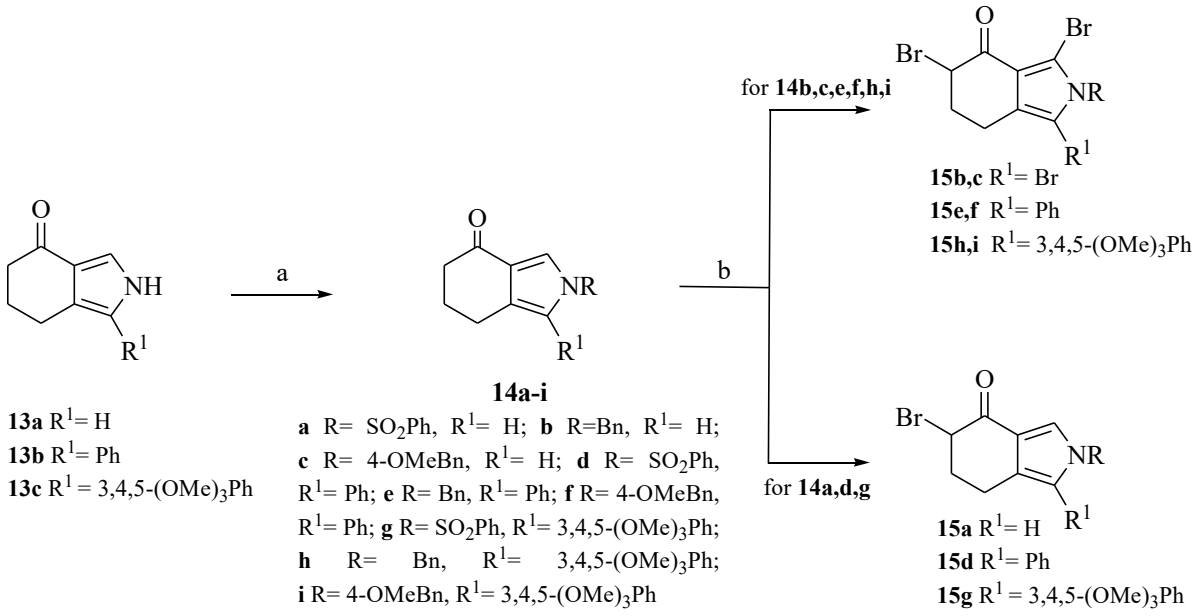

Scheme 1. Synthesis of [1,3]thiazolo[4,5-*e*]isoindoles **11a-l** and **12a-s**. Reagents and conditions: (a) NaH, DMF, 0 °C to rt, 1 h, then aralkyl halide at 0 °C to rt, 1-24 h, 60-90%; (b) Br_2, HBr 45%, in AcOH) chloroform:ethanol (1:1), rt, 1 h, 45-78% for compounds **15b,c,e,f,h,i** or pyridine hydrobromide perbromide, THF, rt, 16 h, 79-90% for compounds **15a,d,g**.

With the key intermediates **15** in hand, we explored the reactivity of α-bromoketones towards unsubstituted thiourea to obtain tricyclic 2-amino thiazoles **11a-i** available for further functionalization (Scheme 2). The reaction of compounds **15a-i** with thiourea in the presence of Na_2CO_3 led to isolation of the desired [1,3]thiazolo[4,5-*e*]isoindoles **11a-i** in high yields (80-99%) (Scheme 2, Table 1). Under the same conditions, only bromoketones **15a,d,g** reacted with phenylthiourea to yield the anilino-[1,3]thiazoles **11j-l** (60-97%) (Scheme 2, Table 1). Aminothiazoles **11a-i** were subjected to acylation using acetyl chloride, benzoyl chloride or 4-methoxybenzoyl chloride in the presence of stoichiometric amounts of triethylamine, leading to acyl derivatives **12a-s** (60-87%) (Scheme 2, Table 1).

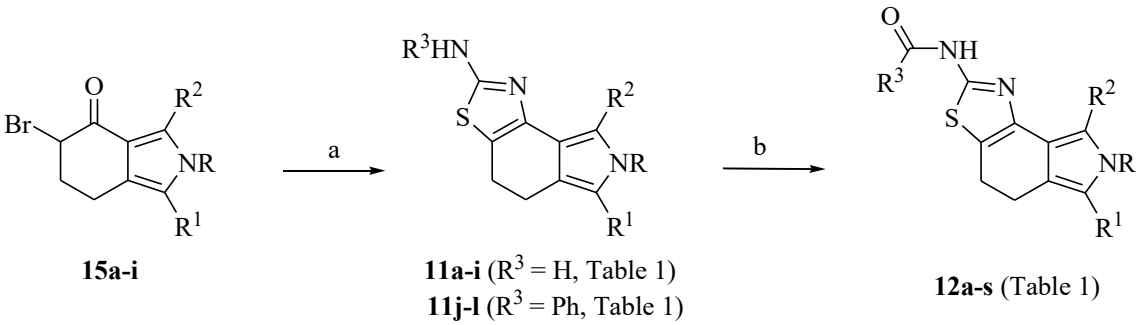

15a-i

11a-i (R^3 = H, Table 1)
11j-l (R^3 = Ph, Table 1)

12a-s (Table 1)

Scheme 2. (a) thiourea or phenylthiourea, Na_2CO_3, DMF, rt, 16 h, 60-99%; (b) acyl chloride, Et_3N, 1,4-dioxane, rt, 16 h, 60-87%.

Table 1. [1,3]Thiazolo[4,5-*e*]isoindol-2-amines of types 11 and 12.

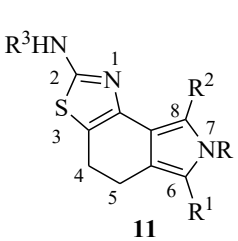

11

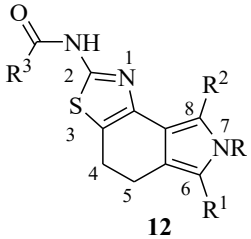

12

Cpd[a]	SM[b]	R	R^1	R^2	R^3	Yield[c]	Cpd[a]	SM[b]	R	R^1	R^2	R^3	Yield[c]
11a	**15a**	SO_2Ph	H	H	H	99%	**12e**	**11e**	Bn	Ph	Br	Ph	68%
11b	**15b**	Bn	Br	Br	H	91%	**12f**	**11f**	4-MeOBn	Ph	Br	Ph	72%
11c	**15c**	4-MeOBn	Br	Br	H	80%	**12g**	**11g**	SO_2Ph	3,4,5-$(MeO)_3$Ph	H	Ph	79%
11d	**15d**	SO_2Ph	Ph	H	H	85%	**12h**	**11h**	Bn	3,4,5-$(MeO)_3$Ph	Br	Ph	60%
11e	**15e**	Bn	Ph	Br	H	95%	**12i**	**11i**	4-MeOBn	3,4,5-$(MeO)_3$Ph	Br	Ph	64%
11f	**15f**	4-MeOBn	Ph	Br	H	95%	**12j**	**11b**	Bn	Br	Br	4-MeOPh	60%
11g	**15g**	SO_2Ph	3,4,5-$(OMe)_3$Ph	H	H	80%	**12k**	**11c**	4-MeOBn	Br	Br	4-MeOPh	64%
11h	**15h**	Bn	3,4,5-$(OMe)_3$Ph	Br	H	95%	**12l**	**11e**	Bn	Ph	Br	4-MeOPh	70%
11i	**15i**	4-MeOBn	3,4,5-$(OMe)_3$Ph	Br	H	96%	**12m**	**11f**	4-MeOBn	Ph	Br	4-MeOPh	64%
11j	**15a**	SO_2Ph	H	H	Ph	88%	**12n**	**11h**	Bn	3,4,5-$(MeO)_3$Ph	Br	4-MeOPh	65%
11k	**15d**	SO_2Ph	Ph	H	Ph	97%	**12o**	**11i**	4-MeOBn	3,4,5-$(MeO)_3$Ph	Br	4-MeOPh	65%
11l	**15g**	SO_2Ph	3,4,5-$(OMe)_3$Ph	H	Ph	60%	**12p**	**11d**	SO_2Ph	Ph	H	Me	72%
12a	**11a**	SO_2Ph	H	H	Ph	67%	**12q**	**11f**	4-MeOBn	Ph	Br	Me	87%
12b	**11b**	Bn	Br	Br	Ph	70%	**12r**	**11g**	SO_2Ph	3,4,5-$(MeO)_3$Ph	H	Me	76%
12c	**11c**	4-MeOBn	Br	Br	Ph	65%	**12s**	**11i**	4-MeOBn	3,4,5-$(MeO)_3$Ph	Br	Me	67%
12d	**11d**	SO_2Ph	Ph	H	Ph	82%							

[a] Compound; [b] Starting Material; [c]The yield obtained at the final reaction step.

2.2 Antiproliferative activity

All compounds were submitted to the National Cancer Institute (NCI) for *in vitro* evaluation at 10^{-5} M against the full NCI panel, including about 60 human cancer cell lines divided into 9 subpanels

(leukemia, non-small-cell lung, colon, central nervous system, melanoma, ovarian, renal, prostate, breast). Compounds **11b**, **11c**, **11g**, **11i**, **12b**, **12s** were further evaluated at five doses (10^{-4}-10^{-8} M).

Table 2. Overview of the results of the NCI *in vitro* human tumor cell line screening for derivatives 11b, 11c, 11g, 11i, 12b, 12s.

Cpd	N° investigated cell lines	N° cell lines with positive GI_{50} values	GI_{50} (μM)	
			Range	MG_MID
11b	56	56	0.53 – 25.70	8.13
11c	56	56	0.41 – 16.00	3.72
11g	57	57	0.22 – 11.20	1.02
11i	57	57	0.21 – 15.10	0.83
12b	57	56	1.20 – 47.30	5.13
12s	56	55	0.61 – 98.50	4.37

An evaluation of the data presented in Table 2 indicated good potential for this class of compounds, which showed growth inhibitory activity in the submicromolar-micromolar range with mean graph mid-point (MG_MID) values between 0.83 and 8.13 μM. The most active compounds of the series were thiazoles **11i** and **11g**, with MG_MID values of 0.83 and 1.02 μM, respectively. Both compounds contained a 3,4,5-trimethoxyphenyl moiety at position 6. Thus, from a structure–activity point of view, the presence of a 3,4,5-trimethoxyphenyl moiety at position 6 is essential for activity, as well as the 4-methoxybenzyl moiety that is present in half of the selected compounds. Moreover, most of them, with the exception of the highly active **11g**, bear a bromine atom at position 8, which seems to play an important role in the modulation of activity. Free amines are generally more active than the corresponding *N*-acyl derivatives, with the only exceptions being one benzoyl (**12b**) and one acetylamino (**12s**) derivative. The *N*-acetylation of the amine at position 2

produced a decrease in activity (compare **11i** MG_MID = 0.83 μM and **12s** MG_MID = 4.37 μM). Moreover, for the *N*-benzyl derivatives, the presence of the free amine produces a slight improvement in activity, with respect to the corresponding benzoyl substituted derivative (compare **11b**, MG_MID = 8.13 μM and **12b** MG_MID = 5.13 μM).

*2.3 Compounds **11i** and **11g** induced arrest of the cell cycle at the G2/M phase*

The effects of a 24 h treatment on cell cycle progression in HeLa cells with different concentrations of the two most active compounds were determined by flow cytometry, following propidium iodide (PI) staining of the cells (Figure 1, Panels A and B). Compounds **11i** and **11g** were tested at 0.1, 1 and 10 μM. Both compounds and, especially, **11g**, caused a significant G2/M arrest in a concentration-dependent manner. At the highest concentration (10 μM), more than 70% of the cells were arrested in G2/M with either compound. The G2/M arrest was accompanied by a significant reduction of G1 phase cells and a more modest reduction of S phase cells.

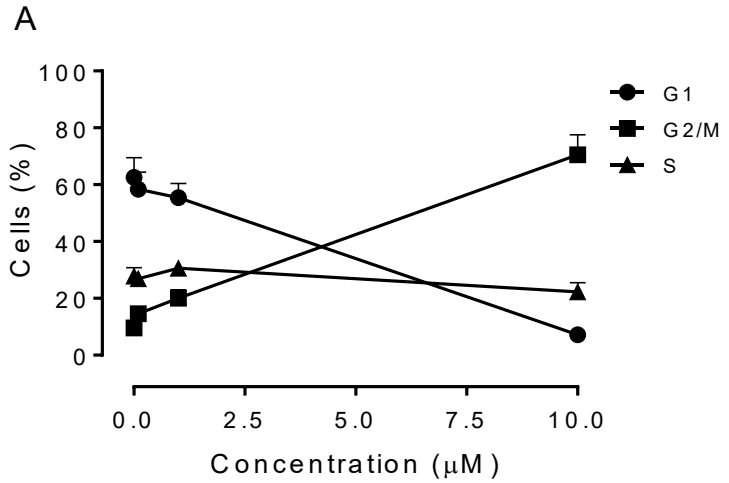

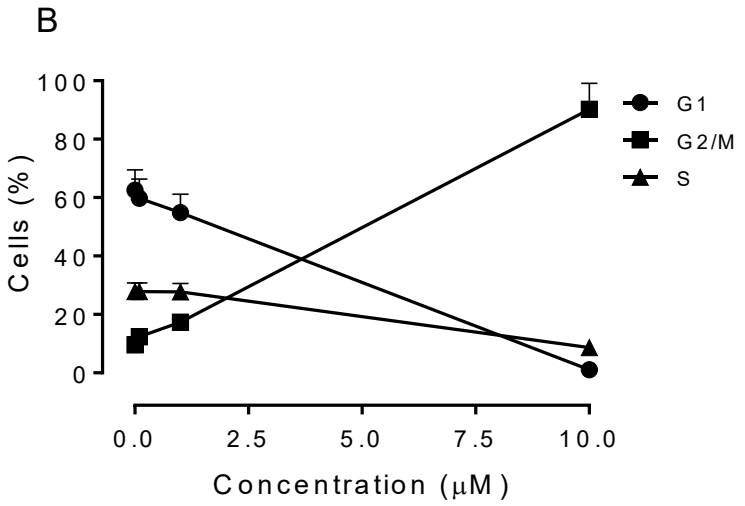

Figure 1. *Percentage of HeLa cells in each phase of the cell cycle following treatment with **11i** (Panel A) or **11g** (Panel B) at the indicated concentrations for 24 h. Cells were fixed and labeled with PI and analyzed by flow cytometry as described in the Experimental Section. Data are presented as mean ± SEM of three experiments.*

*2.4 Compounds **11g** and **11i** induced alterations of spindle assembly checkpoint proteins*

To further investigate the effects of both **11g** and **11i** on the cell cycle, we evaluated their effects on the expression of several proteins involved in regulation of the cell cycle and in spindle assembly. Cyclin B1 is involved in the G2 to M transition as a complex with cdc2, and the activation of the cdc2/cyclin B1 complex through cdc25c-dependent dephosphorylation of phospho-cdc2 and phosphorylation of cyclin B1 triggers cells to enter mitosis [43–45].

As shown in Figure 2, a marked increase of cyclin B1 was observed after a 24 h treatment at the highest concentration used (10 μM) for both compounds. At the same concentration, total cdc25c expression was strongly reduced, in particular for **11g**. Moreover, in good agreement, the expression of phosphorylated cdc2 was also strongly decreased at 10 μM **11g**. Thus, our results showed that, after treatment, cdc2/cyclin B1 complexesfailed to be activated, preventing cells from exiting mitosis, and this should eventually lead to an apoptotic cell death.

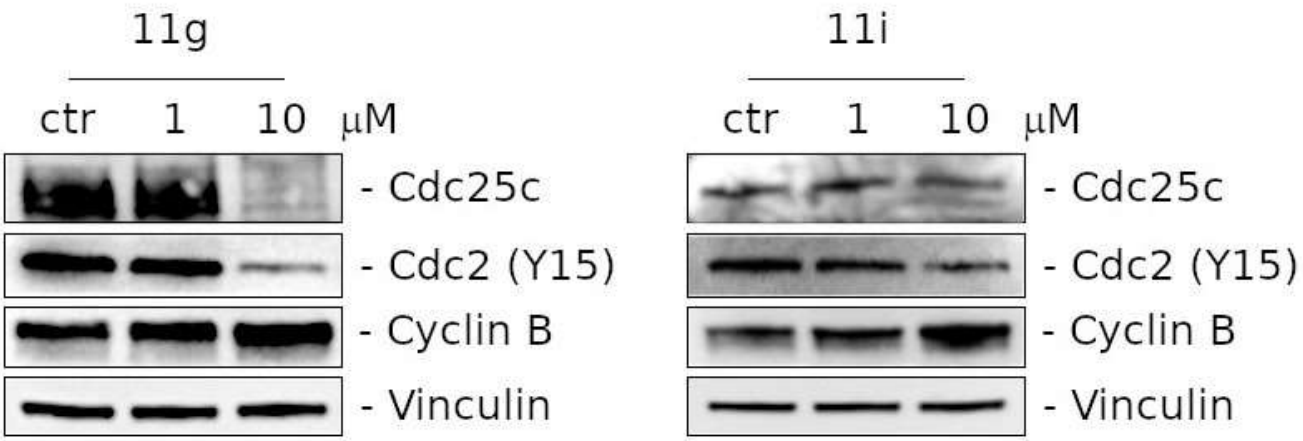

Figure 2. *Effects of **11g** and **11i** on G2/M regulatory proteins. HeLa cells were treated for 24 h with the two compounds at 1 or 10 μM. The cells were harvested and lysed for the detection of cdc25c, p-cdc2^{Y15} and cyclin B1 expression by western blot analysis. To confirm equal protein loading, each membrane was stripped and reprobed with an anti-vinculin antibody.*

*2.5 Compounds **11g** and **11i** induced apoptosis*

To evaluate the mode of cell death induced by compounds **11g** and **11i** in HeLa cells, we used an annexin-V/PI assay. Dual staining for annexin-V and with PI permits discrimination between living cells (annexin-V$^-$/PI$^-$), early apoptotic cells (annexin-V$^+$/PI$^-$), late apoptotic cells (annexin-V$^+$/PI$^+$) and necrotic cells (annexin-V$^-$/PI$^+$). As shown in Figure 3, the cells treated with the test compounds showed a significant accumulation of annexin-V positive cells after a 24 h treatment at 1.0 μM, and apoptosis was even more evident at the higher concentration of both compounds (10 μM). Compound **11g** appeared more potent than **11i** in inducing apoptosis. The percentage of apoptotic cells increased further after 48 h, at which time we also observed a marked increase in necrotic cells, indicating that the compounds at later incubation times induced substantial cell death by both apoptosis and necrosis.

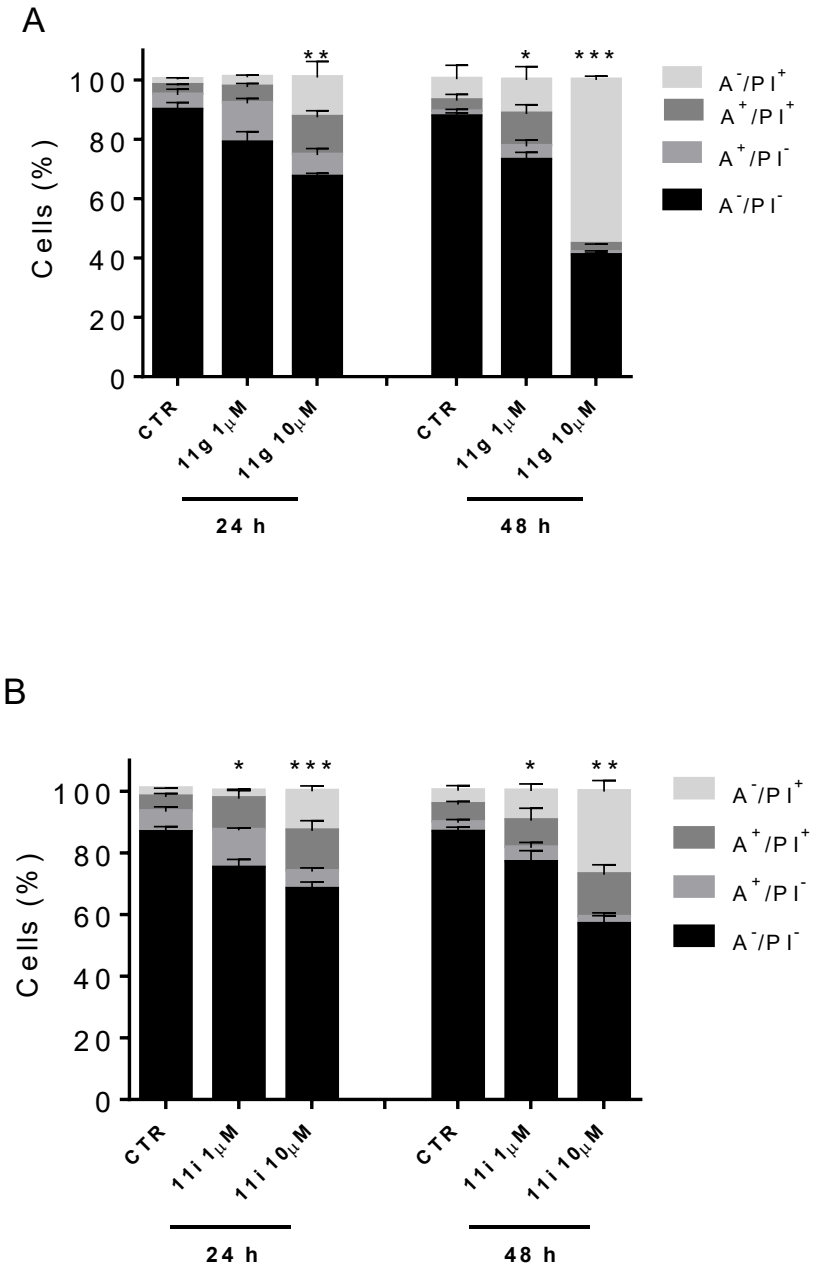

Figure 3. *Flow cytometric analysis of apoptotic cells after treatment of HeLa cells with **11g** (Panel A) or **11i** (Panel B) at the indicated concentrations after incubation for 24 or 48 h. The cells were harvested and labeled with annexin-V-FITC and PI and analyzed by flow cytometry. Data are represented as mean ± SEM of three independent experiments. *p<0.05; **p<0.01; ***p<0.001 vs control.*

*2.6 Compounds **11g** and **11i** induced apoptosis through the mitochondrial pathway*

Mitochondria play an essential role in the propagation of apoptosis [46,47]. At an early stage, apoptotic stimuli alter the mitochondrial transmembrane potential ($\Delta\psi_{mt}$). The reduction of $\Delta\psi_{mt}$ is characteristic of apoptosis and has been observed with both microtubule stabilizing and

destabilizing agents in different cell types [48–51]. HeLa cells treated with **11g** or **11i** (1 and 10 μM) exhibited a significant increase in the percentage of cells with low $\Delta\psi_{mt}$ (Figure 4, Panels A and B). This occurred in a concentration-dependent fashion, and the largest increase was observed with either compound at 10 μM.

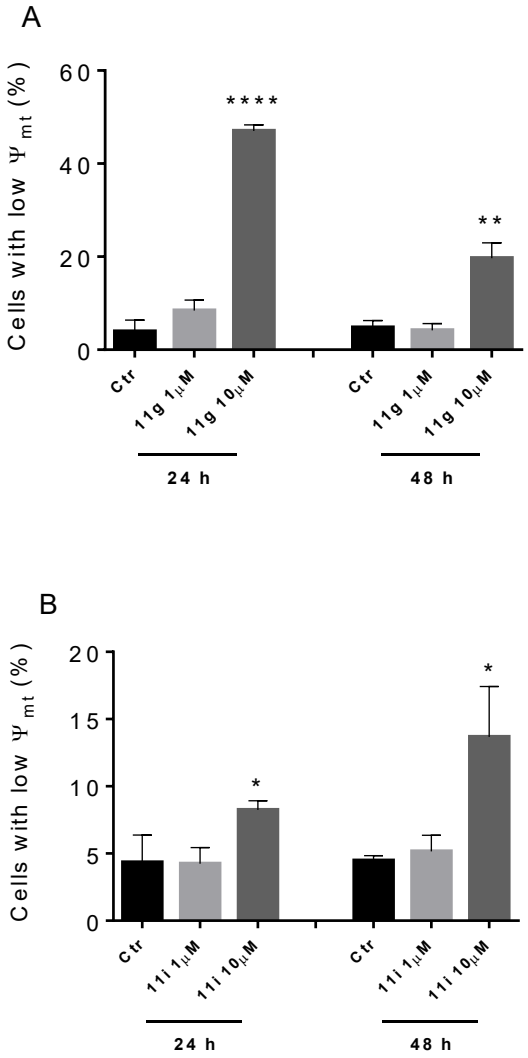

Figure 4. *Assessment of mitochondrial membrane potential ($\Delta\psi_{mt}$) after treatment of HeLa cells with compound **11g** (Panel A) or **11i** (Panel B). Cells were treated with the indicated concentration of compound for 24 or 48 h and then stained with the fluorescent probe JC-1 as described in the Experimental Section. Data are presented as mean ± S.E.M. for three independent experiments. *p<0.05; **p<0.01; ****p<0.0001 vs control.*

*2.7 Compounds **11g** and **11i** induced caspase-9 activation and Poly(ADP-ribose polymerase-1) (PARP) cleavage*

We then analyzed by western blot which apoptotic proteins were involved following treatment with both **11g** and **11i**. HeLa cells were treated with either compounds at 1 or 10 μM for 24 h. As shown in Figure 5, **11g** induced a marked activation of the initiator caspase-9 [52], especially at 10 μM, and at the same concentration we also observed activation of PARP [53]. Similar results were also obtained with **11i**, but both the activation of caspase-9 and the activation of PARP occurred with less intensity. These results are in good agreement with the observed mitochondrial polarization, suggesting that compound **11g** induced apoptosis through the mitochondrial pathway.

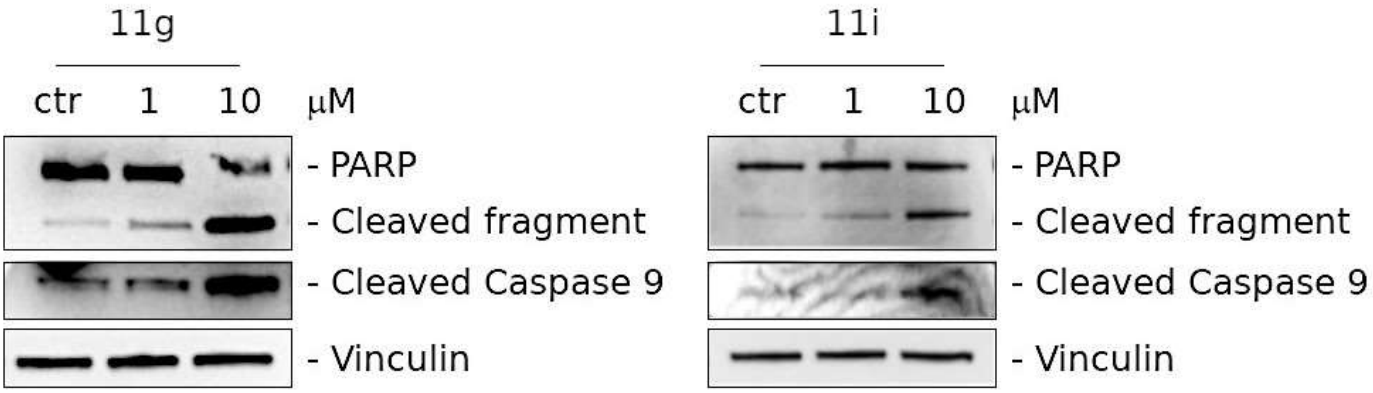

Figure 5. *Western blot analysis of cleaved caspase-9 and PARP after treatment of HeLa cells with **11g** and **11i** at the indicated concentrations for 24 h. To confirm equal protein loading, each membrane was stripped and reprobed with an anti-vinculin antibody.*

2.8 Antitubulin activity

As shown above, compounds **11g** and **11i** showed many effects on cells consistently observed with antitubulin agents. Therefore, these two compounds and several others in the series were evaluated for effects on tubulin assembly, and **11c**, **11i** and **12s** were further evaluated for potential inhibition of the binding of [^{3}H]colchicine to tubulin. They were examined in contemporaneous studies with CA-4 as a positive control. The results obtained are presented in Table 3.

Surprisingly, neither **11g** nor **11i**, as well as **11b** and **12b**, had significant activity as an inhibitor of tubulin assembly. Of the compounds examined, only **11c** and **12s** showed any inhibitory activity. Compared with the potent inhibitory activity of CA-4 (IC_{50} of 1.2 μM), the inhibitory effects of **11c** and **12s** were relatively weak (IC_{50} values of 7.8 and 12 μM, respectively), with **11c** being about 6-fold less active than CA-4.

Three compounds were evaluated for their inhibitory effects on the binding of [^{3}H]colchicine to tubulin. As was originally observed [7], potent inhibition occurred with CA-4 (98% when CA-4 and [^{3}H]colchicine were equimolar at 5.0 μM, with tubulin at 0.5 μM). By contrast, the best inhibitor of

assembly in the present series, compound **11c**, when present at 5.0 μM, only inhibited colchicine binding by 11%. With the inhibitor concentration increased to 50 μM, 60% inhibition occurred with **11c**. Two other compounds, **11i** and **12s**, were also examined at 50 μM and inhibited colchicine binding by 22% and 41%, respectively. Note that within the limited series of **11c**, **12s** and **11i**, there is excellent correlation between effects on tubulin assembly and on [^{3}H]colchicine binding.

Nonetheless, despite the excellent activity of **11g** and **11i** in cellular assays, including cell cycle analysis with accumulation of cells in the G2/M phase, these two compounds did not significantly inhibit tubulin assembly, nor have a significant inhibitory effect on the binding of [^{3}H]colchicine to tubulin. This suggests that the two compounds may be metabolized intracellularly to a more potent entity or that they have an alternate target involved in interfering with mitosis.

Table 3. Antitubulin effects of compounds 11b,11c,11g,11i and 12b,12s in comparison with CA-4

CPD	Inhibition of tubulin assembly	Inhibition of colchicine binding	
	IC_{50} (μM) ± SD	% Inhibition ± SD 5 μM inhibitor	% Inhibition ± SD 50 μM inhibitor
CA-4	1.2 ± 0.08	98 ± 1	-
11b	> 20	-	-
11c	7.8 ± 1	11 ± 6	60 ± 5
11g	> 20	-	-
11i	> 20	-	22 ± 5
12b	> 20	-	-
12s	12 ± 0.07	-	41 ± 5

2.9 Molecular modeling

Since **11c**, **11i** and **12s** had some activity in the tubulin binding assays, their binding modes were investigated through molecular modeling studies. They were docked into the colchicine site, and, for each of them, the pose with the best G-Score (Kcal/mol) was selected and analyzed (Table S2). The most active compound **11c** shared with colchicine the same position in the binding pocket, although it interacted with different residues (Figure S1A-B). Specifically, while colchicine had an H-bond with βV181, **11c** established an H-bond with βA250, through its amine group, and two halogen bonds between the bromine atom at position 6 and the backbone portion of βA317 and

βK352. Conversely, **11i** and **12s** displayed a different binding mode compared to colchicine (Figure S1C-D). In the docking pose of **12s**, the residue βY224 was sandwiched between the 4-methoxybenzyl portion of the ligand and the nitrogenous base of the nonexchangeable GTP bound to α-tubulin, and at the same time it was involved in an internal halogen bond with its own bromine atom. In contrast, **11i** exhibited only a π-cation interaction between its isoindole moiety and the side chain of βK352.

These docked complexes were further subjected to molecular dynamics simulation (MDS) studies with the aim of probing the binding modes and the stabilities of the [1,3]thiazolo[4,5-*e*]isoindole compounds bound to tubulin, using colchicine as the control. Comparative analysis of root-mean-square deviation (RMSD) values, calculated on the heavy atoms of both β-tubulin and the ligands, was performed with respect to the initial structure, by superimposing all ligand-tubulin complexes on the protein backbone (Figure S2). For all complexes, RMSD values showed a stability (Figure S2A) comparable to that of colchicine within 20 ns of the MD trajectories. The most active compound **11c** showed the best stability of the tubulin-ligand structure with respect to all other examined complexes, while **12s** exhibited a colchicine-like RMSD trend. Moreover, the binding mode of all compounds was stable throughout the simulation time, as shown by the RMSD trend of the ligand heavy atoms (Figure S2B). The binding mode of **11c** can be considered the most preserved, with an average RMSD value of 1.6 Å, while the increased RMSD trend at the end of the trajectory of **12s** can be related to a flip of the amidic portion, with the rest of the ligand remaining in the same position as shown in the docking pose.

Protein interactions with each ligand were monitored throughout the simulation, and they have been summarized by taking into account only interactions that occurred more than 15.0% of the entire simulation time (Figure S3). As widely reported in the literature, the most important interactions for colchicine are two H-bonds involving βV181 and βC241 (Figure S3A). During the MDSs, we also observed a series of water bridges that affected the tropolonic portion of the ligand and the β-tubulin residues N349, K352 and T353. Among the [1,3]thiazolo[4,5-*e*]isoindole derivatives, **11i** and **12s** shared a similar pattern of interactions of the phenolic rings. These derivatives established an H-bond between their 3,4,5,-trimethoxyphenyl moiety and βV355, a π-π interaction between their 4-methoxybenzyl moiety and βY224 and several hydrophobic interactions with βA354 and βV328 (Figure S3C-D). Conversely, these two compounds showed a different degree of interaction of their thiazole portion, since the acetyl moiety on the amino group of **12s** allowed further stabilization of the complex, and this provides an explanation for their different activities in inhibiting colchicine binding. Indeed, the binding mode of the more active **12s** was further stabilized by an H-bond between the amide portion and βN101 and by a water-network among the

carbonyl group and βQ11 and βD98 (Figure S3D). On the other hand, **11c** showed a peculiar pattern of interactions, characterized by an H-bond between its amino group and βD251, a π-cation interaction between its phenolic ring and βK352 and several hydrophobic interactions with βL248 and βA316 (Figure S3B).

Finally, the most representative structure of each MDS was analyzed and submitted to MM-GBSA calculation for the evaluation of the binding free energy (ΔG_{bind}) and its different components (Table 4). Among all compounds, **11c** showed the best binding free energy, while **12s** reached a ΔG_{bind} value close to that of colchicine. Moreover, compared to colchicine, **11c** and **12s** exhibited an improvement of the Columbian ($\Delta G_{bind\ Coul}$) and lipophilic terms ($\Delta G_{bind\ Lipo}$) that promote their tubulin binding process (Table 4). Conversely, the van der Waals (ΔG_{bind_vdW}) and solvation ($\Delta G_{bind\ SolvGB}$) components, which play an important role in the tubulin binding of colchicine, have higher values for **11c**, **11i** and **12s**.

Table 4. Binding free energy and related components of the most representative structures of the MDSs.

Compound	ΔG_{bind}	$\Delta G_{bind\ Coul}$	$\Delta G_{bind\ Lipo}$	$\Delta G_{bind\ SolvGB}$	$\Delta G_{bind\ vdW}$
Colchicine	-92.69	-4.90	-43.65	19.27	-67.26
11c	-99.97	-6.48	-54.26	23.97	-63.82
11i	-81.89	-5.76	-41.73	22.15	-57.42
12s	-90.31	-9.97	-48.18	25.65	-58.36

For each most representative cluster of all MDSs, free binding energy values, obtained after MM-GBSA calculation, are shown. Binding free energy and related components are indicated as ΔG_{bind}, $\Delta G_{bind\ Coul}$, $\Delta G_{bind\ Lipo}$, $\Delta G_{bind\ SolvGB}$ and $\Delta G_{bind\ vdW}$ and are expressed as Kcal/mol.

As the docking pose (Figure S2A), the most representative MDs structure of colchicine is characterized by the H-bond between the carbonyl of its tropolonic ring and the backbone of βV181, confirming the validity of our methodology (Figure 6A). Compounds **11i** and **12s** shared the preservation of a similar binding mode with the 3,4,5,-trimethoxyphenyl and the 4-methoxybenzyl moieties facing βV355 and βY224, respectively (Figure 6B-C). In particular, reflecting the experimentally observed inhibition of colchicine binding, **12s** exhibited a further stabilization of its complex by means of an H-bond between its acetyl carbonyl and the side chain of βN101 (Figure 6C). Finally, **11c** established an H-bond between its amine group and the side chain of βD251, also observed in the analysis of the detailed ligand atom interactions with the protein residues during MDSs (Figure 6D). The most representative MD structure of **11c** showed, as

the docking pose, two halogen bonds involving the two bromine atoms with the amide portions of βA317 and βD251.

Thus, we can conclude that **11c** showed the best inhibition of colchicine binding because it bound in the tubulin pocket more similarly to colchicine than the other two compounds, by gaining a better binding free energy, especially for the Columbian and lipophilic components. Moreover, thanks to the acetylation of the amino group on the thiazole ring, **12s** exhibited an improved binding interaction with tubulin as compared to **11i**.

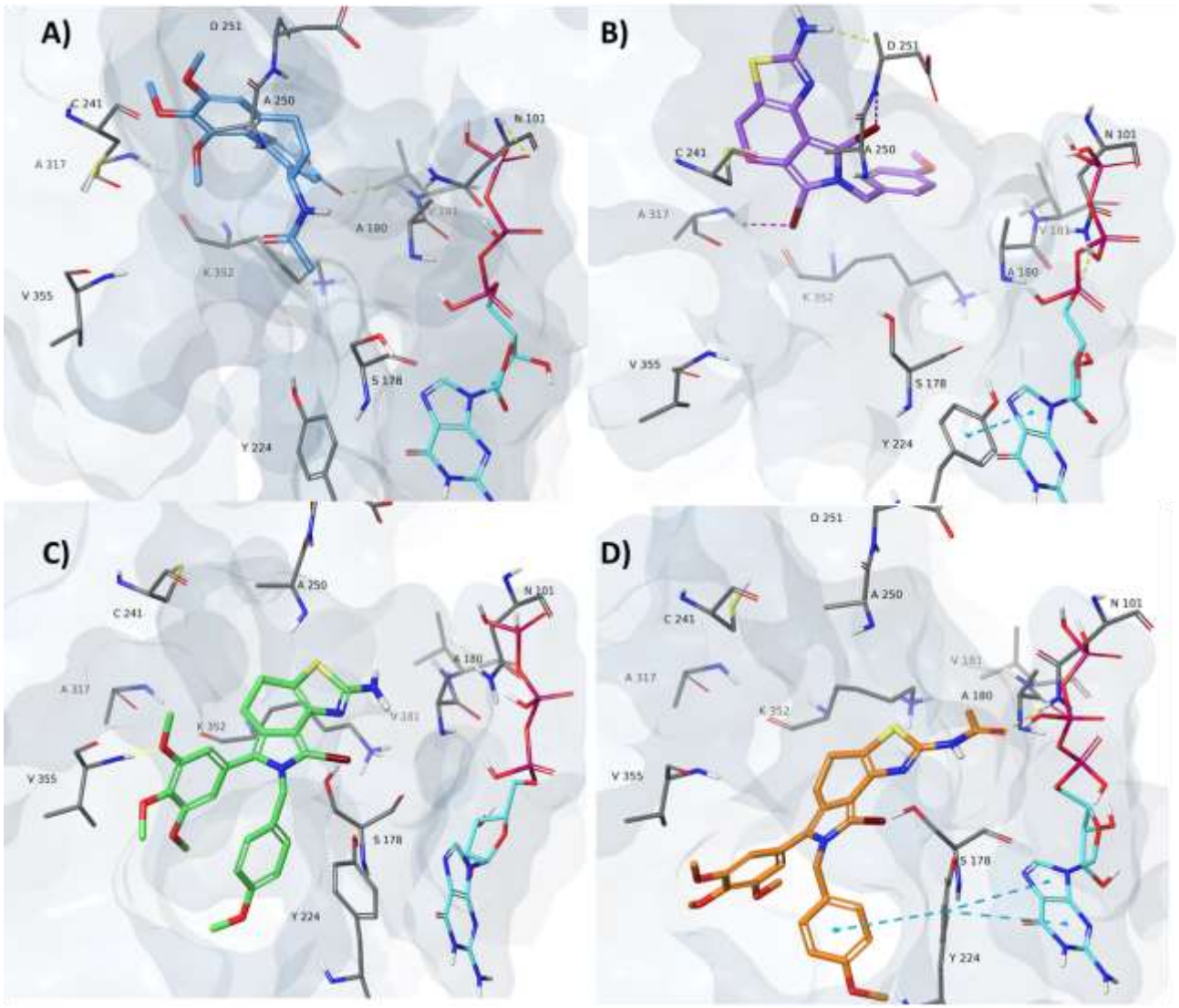

Figure 6. *The most populated cluster of tubulin complexed with **A)** the co-crystallized ligand (colchicine), **B)** **11c**, **C)** **11i** and **D)** **12s** during the whole MD trajectory. Tubulin is shown in faded azure surface, while ligands, GTP and residues involved in the major electrostatic interactions are shown as sticks. Hydrogen and halogen bond interactions are indicated as dashed yellow and purple lines, respectively. Also π-π and π-cation interactions are shown as dashed cyan and green lines, respectively.*

3. Conclusions

In this study, we described the synthesis of a new series of [1,3]thiazolo[4,5-*e*]isoindol-2-amines through a convenient and versatile sequence by annelation of the [1,3]thiazole ring into the isoindole moiety. From a structure–activity point of view, the presence of a 3,4,5-trimethoxyphenyl moiety at position 6, the 4-methoxybenzyl moiety and at least one bromine atom emerged as important structural features for this class of compounds. Although *in vitro* tests indicated that **11i**, followed by **11g**, were the most promising compounds, studies of the mechanism of action highlighted **11g** as the most potent inducer of apoptosis in the HeLa cell line. This compound produced depolarization of the mitochondrial transmembrane potential and activation of caspase-9, which was coupled with terminal events of apoptosis including PARP cleavage. Evaluation of effects on tubulin assembly, however, did not confirm the cellular activity of **11g** and **11i**, possibly due to intracellular metabolism or their interaction with a different target involved in mitosis. Compound **11c**, in contrast, inhibited colchicine binding by 60% at 50 μM as compared with 22% with **11i**, and its superior activity with tubulin was also confirmed by its having the best binding free energy and a binding mode similar to that of colchicine.

4. Experimental Section

4.1. Chemistry. Synthesis and characterization

All melting points were taken on a Büchi melting point M-560 apparatus. IR spectra were determined in bromoform with a Shimadzu FT/IR 8400S spectrophotometer. ^{1}H and ^{13}C NMR spectra were measured at 200 and 50.0 MHz, respectively, in DMSO-d_6 or $CDCl_3$ solution using a Bruker Avance II series 200 MHz spectrometer. Column chromatography was performed with Merck silica gel (230−400 mesh ASTM) or a Büchi Sepacor chromatography module (prepacked cartridge system). Elemental analyses (C, H, N) were within ±0.4% of theoretical values and were performed with a VARIO EL III elemental analyzer. The purity of all the tested compounds was >95%, determined by HPLC (Agilent 1100 series).

Compounds **13a-c**, **14b,c,e,f,i** were prepared according to our published procedures [36,40–42].

*5.1.1. General procedure for the preparation of 2-substituted-2,5,6,7-tetrahydro-4H-isoindol-4-ones (**14a,d,g,h**)*

To a solution of **13a-c** (9 mmol) in anhydrous DMF (17 mL), NaH (0.24 g, 10 mmol) was added at 0 °C, and the reaction mixture was stirred at room temperature for 1 h. Then the suitable aralkyl halide (13.5 mmol) was added at 0 °C, and the reaction mixture was stirred at room temperature

until the reaction was complete (TLC). Then the reaction mixture was poured onto crushed ice. The precipitate was collected by filtration and dried. If there was no precipitate, the solution was extracted with DCM (3 x 50 mL). The combined organic layers were dried (Na_2SO_4), and the solvent was removed under reduced pressure. The crude product was purified by column chromatography using DCM as eluting solvent.

*5.1.1.1 2-(Phenylsulfonyl)-2,5,6,7-tetrahydro-4H-isoindol-4-one (**14a**).* This compound was obtained from reaction of **13a** with benzenesulfonyl chloride after 3 h. Pale brown solid; yield 70%; mp: 115.4–116.2 °C; IR cm^{-1}: 1664 (CO); ^{1}H NMR (DMSO-d_6, 200 MHz, ppm): δ 1.84–1.98 (m, 2H, CH_2), 2.34–2.47 (m, 2H, CH_2), 2.50–2.68 (m, 2H, CH_2), 7.27 (d, 1H, *J* = 1.5 Hz, H-1), 7.60–7.90 (m, 4H, H-3', H-4', H-5'and H-3), 8.06–8.15 (m, 2H, H-2' and H-6'); ^{13}C NMR (DMSO-d_6, 50 MHz, ppm): δ 20.7, 23.6, 39.0, 116.4, 120.8, 125.2, 127.3, 129.1, 130.1, 135.1, 137.3, 194.4. Anal Calcd. for $C_{14}H_{13}NO_3S$: C, 61.07; H, 4.76; N, 5.09. Found: C, 60.98; H, 4.62; N, 4.94.

*5.1.1.2. 2-(Benzenesulfonyl)-1-phenyl-2,5,6,7-tetrahydro-4H-isoindol-4-one (**14d**).* This compound was obtained from reaction of **13b** with benzenesulfonyl chloride after 24 h. Pale brown solid; yield 76%; mp 150–151 °C; IR cm^{-1}: 1674 (CO); ^{1}H NMR (DMSO-d_6, 200 MHz, ppm): δ 1.82–1.94 (m, 2H, CH_2), 2.34 (t, 2H, *J*= 6.2 Hz, CH_2), 2.44 (t, 2H, *J*= 6.2 Hz, CH_2), 7.05–7.10 (m, 2H, Ar), 7.32–7.56 (m, 7H, Ar), 7.68–7.76 (m, 1H, Ar), 7.98 (s, 1H, H-3); ^{13}C NMR (DMSO-d_6, 50 MHz, ppm): δ 20.7, 23.5, 39.0, 122.4, 123.0, 127.2, 127.7, 128.3, 128.8, 128.9, 129.3, 129.7, 131.1, 135.0, 137.0, 194.4. Anal calcd for $C_{20}H_{17}NO_3S$: C, 68.36; H, 4.88; N, 3.99. Found: C, 68.54; H, 4.73; N, 4.06.

*5.1.1.3. 2-(Benzenesulfonyl)-1-(3,4,5-trimethoxyphenyl)-2,5,6,7-tetrahydro-4H-isoindol-4-one (**14g**).* This compound was obtained from reaction of **13c** with benzenesulfonyl chloride after 24 h. Pale brown solid; yield 60%; mp 113–114 °C; IR cm^{-1}: 1676 (CO); ^{1}H NMR (DMSO-d_6, 200 MHz, ppm): δ 1.84–1.97 (m, 2H, CH_2), 2.37–2.47 (m, 4H, 2 x CH_2), 3.65 (s, 6H, 2 x CH_3), 3.73 (s, 3H, CH_3), 6.29 (s, 2H, H-2" and H-6"), 7.45–7.57 (m, 4H, Ar), 7.68–7.77 (m, 1H, Ar), 7.96 (s, 1H, H-3); ^{13}C NMR (DMSO-d_6, 50 MHz, ppm): δ 20.7, 23.5, 39.1, 55.8, 60.1, 108.8, 122.0, 122.6, 123.9, 127.3, 127.9, 129.2, 129.6, 134.9, 136.9, 137.9, 152.1, 194.4. Anal calcd for $C_{23}H_{23}NO_6S$: C, 62.57; H, 5.25; N, 3.17. Found: C, 62.69; H, 5.13; N, 3.08.

*5.1.1.4. 2-Benzyl-1-(3,4,5-trimethoxyphenyl)-2,5,6,7-tetrahydro-4H-isoindol-4-one (**14h**).* This compound was obtained from reaction of **13c** with benzyl bromide after 3 h. White solid; yield 76%; mp 146–147 °C; IR cm^{-1}: 1653 (CO); ^{1}H NMR (DMSO-d_6, 200 MHz, ppm): δ 1.18–2.03 (m, 2H, CH_2), 2.38 (t, 2H, *J*= 5.7 Hz, CH_2), 2.62 (t, 2H, *J*= 5.7 Hz, CH_2), 3.63 (s, 6H, 2 x CH_3), 3.67 (s, 3H, CH_3), 5.21 (s, 2H, CH_2), 6.47 (s, 2H, H-2" and H-6"), 6.97–7.01 (m, 2H, H-2' and H-6'), 7.20–

7.36 (m, 3H, H3', H-4' and H-5'), 7.56 (s, 1H, H-3); ^{13}C NMR (DMSO-d_6, 50 MHz, ppm): δ 21.5, 24.7, 39.0, 50.7, 55.6, 60.0, 106.9, 120.6, 123.3, 124.4, 126.2, 126.6, 127.3, 128.6, 128.9, 136.8, 138.2, 152.7, 193.8. Anal calcd for $C_{24}H_{25}NO_4$: C, 73.64; H, 6.44; N, 3.58. Found: C, 73.76; H, 6.31; N, 3.44.

*5.1.2. General procedure for the preparation of 5-bromo-2-substituted-2,5,6,7-tetrahydro-4H-isoindol-4-ones (**15b,c,e,f,h,i**)*

To a solution of the suitable ketones **14** (2.2 mmol) in a mixture of anhydrous $HCCl_3$-EtOH (1:1, 6 mL), HBr (45% in AcOH, 9 drops) was added at 0 °C, followed by a solution of Br_2 (0.45 mL, 8.8 mmol) in anhydrous $HCCl_3$, and the reaction mixture was stirred at room temperature for 1 h. Then the reaction mixture was added to a saturated solution of $NaHSO_3$. The two phases were separated, and the aqueous phase was extracted with DCM (3 x 50 mL). The combined organic layers were dried (Na_2SO_4), and the solvent was removed under reduced pressure. The crude product was purified by column chromatography using DCM as eluting solvent.

*5.1.2.1. 2-Benzyl-1,3,5-tribromo-2,5,6,7-tetrahydro-4H-isoindol-4-one (**15b**).* This compound was obtained from reaction of **14b**. Pale brown solid; yield 66%; mp 139–140 °C; IR cm^{-1}: 1677 (CO); ^{1}H NMR (DMSO-d_6, 200 MHz, ppm): δ 2.24–2.38 (m, 2H, CH_2), 2.63–2.75 (m, 2H, CH_2), 4.81 (t, 1H, *J*= 4.0 Hz, CH), 5.34 (s, 2H, CH_2), 7.05–7.15 (m, 2H, H-2' and H-6'), 7.26–7.42 (m, 3H, H-3', H-4' and H-5'); ^{13}C NMR (DMSO-d_6, 50 MHz, ppm): δ 18.9, 31.6, 49.8, 52.5, 101.0, 107.0, 116.5, 125.2, 126.2, 127.7, 128.8, 135.5, 184.5. Anal calcd for $C_{15}H_{12}Br_3NO$: C, 39.00; H, 2.62; N, 3.03. Found: C, 39.15; H, 2.76; N, 2.91.

*5.1.2.2. 1,3,5-Tribromo-2-(4-methoxybenzyl)-2,5,6,7-tetrahydro-4H-isoindol-4-one (**15c**).* This compound was obtained from reaction of **14c**. Pale brown solid; yield 75%; mp 109–110 °C; IR cm^{-1}: 1675 (CO); ^{1}H NMR (DMSO-d_6, 200 MHz, ppm): δ 2.26–2.45 (m 2H, CH_2), 2.51–2.68 (m, 2H, CH_2), 3.73 (s, 3H, CH_3), 4.81 (t, 1H, *J*= 3.9 Hz, CH), 5.26 (s, 2H, CH_2), 6.93 (d, 2H, *J*= 8.7 Hz, H-3' and H-5'), 7.05 (d, 2H, *J*= 8.7 Hz, H-2' and H-6'); ^{13}C NMR (DMSO-d_6, 50 MHz, ppm): δ 18.9, 31.6, 49.3, 52.5, 55.1, 100.9, 106.8, 114.2, 116.5, 125.1, 127.3, 127.8, 158.7, 184.4. Anal calcd for $C_{16}H_{14}Br_3NO_2$: C, 39.06; H, 2.87; N, 2.85. Found: C, 38.98; H, 2.99; N, 2.73.

*5.1.2.3. 2-Benzyl-3,5-dibromo-1-phenyl-2,5,6,7-tetrahydro-4H-isoindol-4-one (**15e**).* This compound was obtained from reaction of **14e**. Pale brown solid; yield 70%; mp 156–157 °C; IR cm^{-1}: 1669 (CO); ^{1}H NMR (DMSO-d_6, 200 MHz, ppm): δ 2.22–2.40 (m, 2H, CH_2), 2.63–2.84 (m, 2H, CH_2), 4.83 (t, 1H, *J*= 4.0 Hz, CH), 5.24 (s, 2H, CH_2), 6.86 (t, 2H, *J*= 6.4 Hz, Ar), 7.26–7.41 (m, 8H, Ar); ^{13}C NMR (DMSO-d_6, 50 MHz, ppm): δ 18.7, 32.7, 48.8, 53.2, 108.0, 115.6, 123.1, 125.7,

127.4, 128.4, 128.7, 128.8, 129.8, 130.0, 131.1, 136.5, 185.2. Anal calcd for $C_{21}H_{17}Br_2NO$: C, 54.93; H, 3.73; N, 3.05. Found: C, 54.79; H, 3.58; N, 3.26.

*5.1.2.4. 3,5-Dibromo-2-(4-methoxybenzyl)-1-phenyl-2,5,6,7-tetrahydro-4H-isoindol-4-one (**15f**).* This compound was obtained from reaction of **14f**. Pale brown solid; yield 63%; mp 156–157 °C; IR cm^{-1}: 1665 (CO); ^1H NMR (DMSO-d_6, 200 MHz, ppm): δ 2.22–2.45 (m, 2H, CH_2), 2.56–2.85 (m, 2H, CH_2), 3.70 (s, 3H, CH_3), 4.82 (t, 1H, *J*= 4.4 Hz, CH), 5.17 (s, 2H, CH_2), 6.77 (d, 2H, *J*= 9.0 Hz, H-3' and H-5'), 6.85 (d, 2H, *J*= 9.0 Hz, H-2' and H-6'), 7.30–7.47 (m, 5H, Ar); ^{13}C NMR (DMSO-d_6, 50 MHz, ppm): δ 18.6, 32.6, 48.2, 53.2, 55.0, 107.9, 114.0, 115.6, 123.1, 127.2, 128.3, 128.4, 128.8, 129.8, 130.1, 131.0, 158.4, 185.1. Anal calcd for $C_{22}H_{19}Br_2NO_2$: C, 54.01; H, 3.91; N, 2.86. Found: C, 54.13; H, 4.02; N, 2.95.

*5.1.2.5. 2-Benzyl-3,5-dibromo-1-(3,4,5-trimethoxyphenyl)-2,5,6,7-tetrahydro-4H-isoindol-4-one (**15h**).* This compound was obtained from reaction of **14h**. Pale brown solid, yield 78%; mp 173–174 °C; IR cm^{-1}: 1669 (CO); ^1H NMR (DMSO-d_6, 200 MHz, ppm): δ 2.18–2.34 (m, 2H, CH_2), 2.60–2.89 (m, 2H, CH_2), 3.57 (s, 3H, CH_3), 3.59 (s, 3H, CH_3), 3.67 (s, 3H, CH_3), 4.83 (t, 1H, *J*= 4.0 Hz, CH), 5.24 (s, 2H, CH_2), 6.50 (s, 2H, H-2" and H-6"), 6.93–6.97 (m, 2H, H-2' and H-6'), 7.23–7.40 (m, 3H, H-3', H-4' and H-5'); ^{13}C NMR (DMSO-d_6, 50 MHz, ppm): δ 18.6, 32.7, 47.7, 53.1, 55.6, 60.0, 107.2, 108.0, 115.4, 122.9, 125.3, 125.7, 127.3, 128.8, 136.7, 136.9, 137.3, 152.8, 185.2. Anal calcd for $C_{24}H_{23}Br_2NO_4$: C, 52.48; H, 4.22; N, 2.55. Found: C, 52.35; H, 4.09; N, 2.64.

*5.1.2.6. 3,5-Dibromo-2-[(4-methoxyphenyl)methyl]-1-(3,4,5-trimethoxyphenyl)-2,5,6,7-tetrahydro-4H-isoindol-4-one (**15i**).* This compound was obtained from reaction of **14i**. Pale brown solid; yield 45%; mp 174–175 °C; IR cm^{-1}: 1669 (CO); ^1H NMR (DMSO-d_6, 200 MHz, ppm): δ 2.25–2.43 (m, 2H, CH_2), 2.67–2.85 (m, 2H, CH_2), 3.63 (s, 6H, 2 x CH_3), 3.68 (s, 3H, CH_3), 3.70 (s, 3H, CH_3), 4.81 (t, 1H, *J*= 4.0 Hz, CH), 5.17 (s, 2H, CH_2), 6.52 (s, 2H, H-2" and H-6"), 6.81–6.91 (m, 4H, H-2', H-3', H-5' and H-6'); ^{13}C NMR (DMSO-d_6, 50 MHz, ppm): δ 18.4, 32.7, 47.2, 53.0, 55.1, 55.7, 60.0, 107.2, 112.9, 114.1, 119.9, 121.9, 125.1, 127.3, 128.4, 129.2, 137.4, 152.9, 158.5, 185.0. Anal calcd for $C_{25}H_{25}Br_2NO_5$: C, 51.83; H, 4.35; N, 2.42. Found: C, 51.99; H, 4.46; N, 2.29.

*5.1.3. General procedure for the preparation of 5-bromo-2-benzenesulfonyl-2,5,6,7-tetrahydro-4H-isoindol-4-ones (**15a,d,g**)*

To a solution of suitable ketones **14** (2.3 mmol) in anhydrous THF (11 mL) a solution of pyridinium bromide-perbromide (0.73 g, 2.3 mmol) in anhydrous THF (8 mL) was added dropwise at 0 °C, and the reaction mixture was stirred at room temperature for 16 h. Then the precipitate was removed from the reaction mixture by filtration, and the filtrate was evaporated under reduced pressure. The

residue was dissolved in DMC, and the resulting solution was stirred with a 5% aqueous solution of $NaHCO_3$ (15 mL). The organic phase was separated and dried (Na_2SO_4), and the solvent was removed under reduced pressure. The crude product was purified by column chromatography using DCM as eluting solvent.

*5.1.3.1. 5-Bromo-2-(phenylsulfonyl)-2,5,6,7-tetrahydro-4H-isoindol-4-one (**15a**).* This compound was obtained from reaction of **14a**. White solid; yield 90%; mp: 134–135 °C; IR cm^{-1}: 1683 (CO); ^{1}H NMR (DMSO-d_6, 200 MHz, ppm): δ 2.15–2.50 (m, 2H, CH_2), 2.65–2.78 (m, 2H, CH_2), 4.85–4.85 (m, 1H, CH), 7.34 (s, 1H, H-1), 7.65 - 7.90 (m, 3H, H-3', H-4' and H-5'), 8.04 (s, 1H, H-3), 8.08–8.19 (m, 2H, H-2' and H-6'); ^{13}C NMR (DMSO-d_6, 50 MHz, ppm): δ 17.9, 32.3, 52.3, 116.8, 122.1, 123.1, 127.1, 127.4, 130.2, 135.4, 137.0, 186.7. Anal. Calcd. for $C_{14}H_{12}BrNO_3S$: C, 47.47; H, 3.41; N, 3.95. Found: C, 47.56; H, 3.57; N, 4.03.

*5.1.3.2. 2-(Benzenesulfonyl)-5-bromo-1-phenyl-2,5,6,7-tetrahydro-4H-isoindol-4-one (**15d**).* This compound was obtained from reaction of **14d**. White solid; yield 82%; mp 144–145 °C; IR cm^{-1}: 1681 (CO); ^{1}H NMR (DMSO-d_6, 200 MHz, ppm): δ 2.19–2.40 (m, 4H, 2 x CH_2), 4.88 (t, 1H, *J*= 3.0 Hz, CH), 7.07–7.11 (m, 2H, Ar), 7.33–7.57 (m, 7H, Ar), 7.70–7.79 (m, 1H, Ar), 8.16 (s, 1H, H-3); ^{13}C NMR (DMSO-d_6, 50 MHz, ppm): δ 18.0, 32.3, 52.3, 120.0, 124.6, 126.3, 127.4, 127.9, 128.5, 129.0, 129.5, 129.7, 131.2, 135.2, 136.7, 186.8. Anal calcd for $C_{20}H_{16}BrNO_3S$: C, 55.82; H, 3.75; N, 3.25. Found: C, 55.98; H, 3.63; N, 3.09.

*5.1.3.3. 2-(Benzenesulfonyl)-5-bromo-1-(3,4,5-trimethoxyphenyl)-2,5,6,7-tetrahydro-4H-isoindol-4-one (**15g**).* This compound was obtained from reaction of **14g**. White solid; yield 79%; mp 134–135 °C; IR cm^{-1}: 1682 (CO); ^{1}H NMR (DMSO-d_6, 200 MHz, ppm): δ 2.19–2.59 (m, 4H, 2 x CH_2), 3.65 (s, 6H, 2 x CH_3), 3.74 (s, 3H, CH_3), 4.87 (t, 1H, *J*= 5.6 Hz, CH), 6.31 (s, 2H, H-2" and H-6"), 7.52–7.76 (m, 5H, H-2', H-3', H-4', H-5' and H-6'), 8.14 (s, 1H, H-3); ^{13}C NMR (DMSO-d_6, 50 MHz, ppm): δ 17.9, 32.3, 52.2, 55.8, 60.1, 108.8, 119.5, 123.5, 124.2, 126.0, 127.5, 129.4, 129.7, 135.1, 136.6, 138.0, 152.2, 186.8. Anal calcd for $C_{23}H_{22}BrNO_6S$: C, 53.08; H, 4.26; N, 2.69. Found: C, 52.95; H, 4.17; N, 2.80.

*5.1.4. General procedure for the preparation of 5,7-dihydro-4H-[1,3]thiazolo[4,5-e]isoindoles (**11a-l**)*

To a solution of **15a-i** (0.5 mmol) in anhydrous DMF (5 mL), Na_2CO_3 (0.11 g, 1 mmol) and thiourea or phenyl thiourea (1 mmol) were added, and the reaction mixture was stirred at room temperature for 16 h. Then the reaction mixture was poured onto crushed ice. The precipitate was collected by filtration, dried and recrystallized from methanol.

*5.1.4.1. 7-(Phenylsulfonyl)-5,7-dihydro-4H-[1,3]thiazolo[4,5-e]isoindol-2-amine (**11a**).* This compound was obtained from reaction of **15a**. Light gray solid; yield 99%; mp 209–210 °C; IR cm^{-1}: 3407–3276 (NH_2); ^1H NMR (DMSO-d_6, 200 MHz, ppm): δ 2.65–2.75 (m, 4H, 2 x CH_2), 6.91 (s, 2H, NH_2), 7.03 (d, 1H, *J* = 2.0 Hz, H-6), 7.11 (d, 1H, *J* = 2.0 Hz, H-8), 7.55–7.80 (3H, m, H-3', H-4' and H-5'), 7.95 (d, 2H, *J*= 7.0 Hz, H-2' and H-6'); ^{13}C NMR ((DMSO-d_6, 50 MHz, ppm): δ 20.1, 21.6, 111.8, 116.9, 117.2, 123.2, 124.6, 126.6, 129.8, 134.3, 138.1, 139.3, 166.9. Anal. Calcd. for $C_{15}H_{13}N_3O_2S_2$: C, 54.36; H, 3.95; N, 12.68. Found: C, 54.22; H, 3.75; N, 12.78.

*5.1.4.2. 7-Benzyl-6,8-dibromo-5,7-dihydro-4H-[1,3]thiazolo[4,5-e]isoindol-2-amine (**11b**).* This compound was obtained from reaction of **15b**. Light gray solid; yield 91%; mp 74–75 °C; IR cm^{-1}: 3323–3373 (NH_2); ^1H NMR (DMSO-d_6, 200 MHz, ppm): δ 2.60 (t, 2H, *J*= 6.4 Hz, CH_2), 2.73 (t, 2H, *J*= 6.4 Hz, CH_2), 5.22 (s, 2H, CH_2), 6.91 (s, 2H, NH_2), 7.02 (d, 2H, *J*= 6.6 Hz, Ar), 7.22–7.38 (m, 3H, Ar); ^{13}C NMR (DMSO-d_6, 50 MHz, ppm): δ 21.0, 21.5, 48.6, 105.2, 114.2, 114.9, 118.2, 119.6, 125.9, 127.3, 128.6, 137.2, 139.5, 166.4. Anal calcd for $C_{16}H_{13}Br_2N_3S$: C, 43.76; H, 2.98; N, 9.57. Found: C, 43.88; H, 3.09; N, 9.41.

*5.1.4.3. 6,8-Dibromo-7-(4-methoxybenzyl)-5,7-dihydro-4H-[1,3]thiazolo[4,5-e]isoindol-2-amine (**11c**).* This compound was obtained from reaction of **15c**. Light gray solid; yield 80%; mp 175–176 °C; IR cm^{-1}: 3408–3290 (NH_2); ^1H NMR (DMSO-d_6, 200 MHz, ppm): δ 2.63 (t, 2H, *J*= 6.2 Hz, CH_2), 2.75 (t, 2H, *J*= 6.2 Hz, CH_2), 3.71 (s, 3H, CH_3), 5.14 (s, 2H, CH_2), 6.88–7.02 (m, 6H, NH_2 and Ar); ^{13}C NMR (DMSO-d_6, 50 MHz, ppm): δ 21.0, 21.5, 48.6, 55.0, 95.7, 99.7, 114.0, 114.8, 118.2, 119.6, 127.4, 129.0, 139.5, 158.4, 166.3. Anal calcd for $C_{17}H_{15}Br_2N_3OS$: C, 43.52; H, 3.22; N, 8.96. Found: C, 43.39; H, 3.07; N, 9.11.

*5.1.4.4. 6-Phenyl-7-(phenylsulfonyl)-5,7-dihydro-4H-[1,3]thiazolo[4,5-e]isoindol-2-amine (**11d**).* This compound was obtained from reaction of **15d**. Light gray solid; yield 85%; mp 194–195 °C; IR cm^{-1}: 3419–3302 (NH_2); ^1H NMR (DMSO-d_6, 200 MHz, ppm): δ 2.44–2.51 (m, 2H, CH_2), 2.63–2.73 (m, 2H, CH_2), 6.98 (s, 2H, NH_2), 7.16–7.22 (m, 3H, Ar), 7.37–7.54 (m, 7H, H-8 and Ar), 7.67 (t, 1H, *J*= 7.3 Hz, Ar); ^{13}C NMR (DMSO-d_6, 50 MHz, ppm): δ 20.0, 21.4, 114.3, 117.7, 121.9, 124.6, 126.4, 127.5, 128.2, 129.4, 129.9, 130.6, 130.8, 134.2, 137.6, 139.3, 167.0. Anal calcd for $C_{21}H_{17}N_3O_2S_2$: C, 61.89; H, 4.20; N, 10.31. Found: C, 61.72; H, 4.07; N, 10.55.

*5.1.4.5. 7-Benzyl-8-bromo-6-phenyl-5,7-dihydro-4H-[1,3]thiazolo[4,5-e]isoindol-2-amine (**11e**).* This compound was obtained from reaction of **15e**. Light gray solid; yield 95%; mp 94–dec °C; IR cm^{-1}: 3472–3380 (NH_2); ^1H NMR (DMSO-d_6, 200 MHz, ppm): δ 2.65–2.79 (m, 4H, 2 x CH_2), 5.13 (s, 2H, CH_2), 6.84–6.94 (m, 4H, NH_2 and Ar), 7.16–7.45 (m, 8H, Ar); ^{13}C NMR (DMSO-d_6, 50 MHz, ppm): δ 20.7, 22.1, 54.9, 109.9, 114.2, 116.8, 117.8, 125.5, 127.6, 128.4, 128.5, 128.6, 129.3,

129.4, 131.0, 131.1, 138.1, 166.6. Anal calcd for $C_{22}H_{18}BrN_3S$: C, 60.55; H, 4.16; N, 9.63. Found: C, 60.64; H, 4.02; N, 9.75.

*5.1.4.6. 8-Bromo-7-(4-methoxybenzyl)-6-phenyl-5,7-dihydro-4H-[1,3]thiazolo[4,5-e]isoindol-2-amine (**11f**).* This compound was obtained from reaction of **15f**. Light gray solid; yield 95%; mp 75–dec °C; IR cm^{-1}: 3478–3361 (NH_2); ^1H NMR (DMSO-d_6, 200 MHz, ppm): δ 2.62–2.69 (m, 4H, 2 x CH_2), 3.68 (s, 3H, CH_3), 5.07 (s, 2H, CH_2), 6.76 (d, 2H, *J*= 9.0 Hz, H-3' and H-5'), 6.82 (d, 2H, *J*= 9.0 Hz, H-2' and H-6'), 6.90 (s, 2H, NH_2), 7.26–7.45 (m, 5H, H-2", H-3", H-4", H-5" and H-6"); ^{13}C NMR (DMSO-d_6, 50 MHz, ppm): δ 20.8, 22.2, 47.8, 55.0, 97.3, 98.7, 113.9, 114.3, 117.8, 126.9, 127.7, 128.6, 129.5, 130.1, 131.1, 131.3, 140.0, 151.1, 158.2. Anal calcd for $C_{23}H_{20}BrN_3OS$: C, 59.23; H, 4.32; N, 9.01. Found: C, 59.16; H, 4.43; N, 9.22.

*5.1.4.7. 7-(Phenylsulfonyl)-6-(3,4,5-trimethoxyphenyl)-5,7-dihydro-4H-[1,3]thiazolo[4,5-e]isoindol-2-amine (**11g**).* This compound was obtained from reaction of **15g**. Light gray solid; yield 80%; mp 191–192 °C; IR cm^{-1}: 3409–3322 (NH_2); ^1H NMR (DMSO-d_6, 200 MHz, ppm): δ 2.51–2.69 (m, 4H, 2 x CH_2), 3.70 (s, 6H, 2 x CH_3), 3.73 (s, 3H, CH_3), 6.38 (s, 2H, H-2" and H-6"), 6.97 (s, 2H, NH_2), 7.24 (s, 1H, H-8), 7.42–7.72 (m, 5H, H-2', H-3', H-4', H-5' and H-6'); ^{13}C NMR (DMSO-d_6, 50 MHz, ppm): δ 20.0, 21.4, 55.8, 60.1, 108.6, 113.9, 117.5, 121.4, 124.1, 124.9, 126.6, 129.4, 130.4, 134.1, 137.6, 137.7, 139.3, 151.9, 167.0. Anal calcd for $C_{24}H_{23}N_3O_5S_2$: C, 57.93; H, 4.66; N, 8.44. Found: C, 58.05; H, 4.78; N, 8.32.

*5.1.4.8. 7-Benzyl-8-bromo-6-(3,4,5-trimethoxyphenyl)-5,7-dihydro-4H-[1,3]thiazolo[4,5-e]isoindol-2-amine (**11h**).* This compound was obtained from reaction of **15h**. Light gray solid; yield 95%; mp 95–96 °C; IR cm^{-1}: 3465–3377 (NH_2); ^1H NMR (DMSO-d_6, 200 MHz, ppm): δ 2.64–2.83 (s, 4H, 2 x CH_2), 3.57 (s, 6H, 2 x CH_3), 3.66 (s, 3H, CH_3), 5.15 (s, 2H, CH_2), 6.46 (s, 2H, H-2" and H-6"), 6.84–6.98 (m, 4H, H-2', H-6' and NH_2), 7.19–7.36 (m, 3H, H-3', H-4' and H-5'); ^{13}C NMR (DMSO-d_6, 50 MHz, ppm): δ 20.9, 22.1, 48.5, 55.6, 60.0, 97.2, 106.8, 114.4, 116.9, 117.6, 125.6, 126.4, 126.6, 126.9, 128.5, 131.0, 136.9, 138.7, 152.6, 166.1. Anal calcd for $C_{25}H_{24}BrN_3O_3S$: C, 57.04; H, 4.60; N, 7.98. Found: C, 56.96; H, 4.79; N, 8.09.

*5.1.4.9. 8-Bromo-7-(4-methoxybenzyl)-6-(3,4,5-trimethoxyphenyl)-5,7-dihydro-4H-[1,3]thiazolo[4,5-e]isoindol-2-amine (**11i**).* This compound was obtained from reaction of **15i**. Light gray solid; yield 96%; mp 182–183 °C; IR cm^{-1}: 3459–3352 (NH_2); ^1H NMR (DMSO-d_6, 200 MHz, ppm): δ 2.67–2.78 (m, 4H, 2 x CH_2), 3.61 (s, 6H, 2 x CH_3), 3.67 (s, 3H, CH_3), 3.70 (s, 3H, CH_3), 5.08 (s, 2H, CH_2), 6.48 (s, 2H, H-2" and H-6"), 6.83–6.87 (m, 6H, H-2', H-3', H-5', H-6' and NH_2); ^{13}C NMR (DMSO-d_6, 50 MHz, ppm): δ 21.7, 22.1, 46.7, 55.1, 55.7, 60.0, 97.1, 106.9, 109.8, 113.9, 116.6, 117.9, 126.9, 129.2, 130.3, 136.9, 152.6, 152.7, 158.2, 158.3, 166.1. Anal calcd for $C_{26}H_{26}BrN_3O_4S$: C, 56.12; H, 4.71; N, 7.55. Found: C, 56.29; H, 4.59; N, 7.42.

*5.1.4.10. N-phenyl-7-(phenylsulfonyl)-5,7-dihydro-4H-[1,3]thiazolo[4,5-e]isoindol-2-amine (**11j**).* This compound was obtained from reaction of **15a**. Light gray solid; yield 88%; mp 193–194 °C; IR cm^{-1}: 3220 (NH); ^1H NMR (DMSO-d_6, 200 MHz, ppm): δ 2.72–2.85 (m, 4H, 2 x CH_2), 6.91–7.46 (m, 6H, Ar), 7.37–7.54 (m, 4H, Ar), 7.97–8.03 (m, 2H, Ar), 10.2 (s, 1H, NH); ^{13}C NMR (DMSO-d_6, 50 MHz, ppm): δ 20.0, 21.4, 116.8, 117.0, 118.4, 122.7, 122.8, 124.4, 126.7, 128.6, 128.9, 129.8, 134.4, 138.1, 139.7, 141.1, 161.7. Anal calcd for $C_{21}H_{17}N_3O_2S_2$: C, 61.89; H, 4.20; N, 10.31. Found: C, 61.98; H, 4.35; N, 10.22.

*5.1.4.11. N,6-diphenyl-7-(phenylsulfonyl)-5,7-dihydro-4H-[1,3]thiazolo[4,5-e]isoindol-2-amine (**11k**).* This compound was obtained from reaction of **15d**. Light gray solid; yield 97%; mp 113–114 °C; IR cm^{-1}: 3386 (NH); ^1H NMR ($CDCl_3$, 200 MHz, ppm): δ 2.58 (t, 2H, *J*= 6.6 Hz, CH_2), 2.78 (t, 2H, *J*= 6.6 Hz, CH_2), 7.08–7.47 (m, 15H, Ar), 7.59 (s, 1H, H-8), 8.59 (s, 1H, NH); ^{13}C NMR ($CDCl_3$, 50 MHz, ppm): δ 20.4, 22.2, 115.6, 118.3, 118.8, 120.7, 123.0, 124.2, 127.1, 127.5, 128.3, 128.7, 129.5, 130.2, 130.8, 131.4, 133.4, 138.5, 140.3, 140.5, 163.6. Anal calcd for $C_{27}H_{21}N_3O_2S_2$: C, 67.06; H, 4.38; N, 8.69. Found: C, 67.24; H, 4.17; N, 8.55.

*5.1.4.12. N-phenyl-7-(phenylsulfonyl)-6-(3,4,5-trimethoxyphenyl)-5,7-dihydro-4H-[1,3]thiazolo[4,5-e]isoindol-2-amine (**11l**).* This compound was obtained from reaction of **15g**. Light gray solid; yield 60%; mp 121–122 °C; IR cm^{-1}: 3176 (NH); ^1H NMR ($CDCl_3$, 200 MHz, ppm): δ 2.64 (t, 2H, *J*= 6.6 Hz, CH_2), 2.82 (t, 2H, *J* = 6.6 Hz, CH_2), 3.77 (s, 6H, 2 x CH_3), 3.92 (s, 3H, CH_3), 6.34 (s, 2H, H-2" and H-6"), 7.28–7.50 (m, 10H, Ar), 7.66 (s, 1H, H-8), 8.11 (s, 1H, NH); ^{13}C NMR ($CDCl_3$, 50 MHz, ppm): δ 20.5, 22.3, 56.1, 61.0, 108.9, 115.5, 118.2, 118.7, 123.7, 125.2, 127.4, 128.7, 129.5, 129.7, 130.5, 133.4, 133.8, 138.1, 138.6, 140.2, 152.2, 163.3, 165.3. Anal calcd for $C_{30}H_{27}N_3O_5S_2$: C, 62.81; H, 4.74; N, 7.32. Found: C, 62.98; H, 4.59; N, 7.19.

*5.1.5. General procedure for the preparation of N-(7-substituted-5,7-dihydro-4H-[1,3]thiazolo[4,5-e]isoindol-2-yl)amides (**12a-s**)*

To a solution of **11a-i** (0.46 mmol) in anhydrous 1,4-dioxane (3 mL), Et_3N (0.07 mL, 0.51 mmol) and the suitable acyl chloride (0.69 mmol) were added, and the reaction mixture was stirred at room temperature for 16 h. Then the reaction mixture was poured onto crushed ice. The precipitate was collected by filtration, dried and purified by column chromatography using DCM as eluting solvent.

*5.1.5.1. N-[7-(phenylsulfonyl)-5,7-dihydro-4H-[1,3]thiazolo[4,5-e]isoindol-2-yl]benzamide (**12a**).* This compound was obtained from reaction of **11a** with benzoyl chloride. White solid; yield 67%; mp 128–129 °C; IR cm^{-1}: 3405 (NH), 1669 (CO); ^1H NMR (DMSO-d_6, 200 MHz, ppm): δ 2.76 (t, 2H, *J*= 6.9 Hz, CH_2), 2.91 (t, 2H, *J*= 6.9 Hz, CH_2), 7.22 (d, 2H, *J*= 5.9 Hz, Ar), 7.51–7.79 (m, 6H, Ar), 8.00 (d, 2H, *J*= 7.0 Hz, Ar), 8.11 (d, 2H, *J*= 6.8 Hz, Ar), 12.69 (s, 1H, NH); ^{13}C NMR (DMSO-d_6, 50 MHz, ppm): δ 19.9, 21.4, 112.0, 117.3, 122.5, 123.9, 124.8, 126.7, 128.1, 128.6, 129.9,

131.9, 132.6, 134.5, 138.0, 138.8, 156.8, 164.8. Anal calcd for $C_{22}H_{17}N_3O_3S_2$: C, 60.67; H, 3.93; N, 9.65. Found: C, 60. 52; H, 4.04; N, 9.52.

*5.1.5.2. N-(7-benzyl-6,8-dibromo-5,7-dihydro-4H-[1,3]thiazolo[4,5-e]isoindol-2-yl)benzamide (**12b**).* This compound was obtained from reaction of **11b** with benzoyl chloride. Dark yellow solid; yield 70%; mp 255–256 °C; IR cm^{-1}: 3539 (NH), 1649 (CO); ^1H NMR ($CDCl_3$, 200 MHz, ppm): δ 2.80 (t, 2H, *J*= 7.1 Hz, CH_2), 3.00 (t, 2H, *J*= 7.1 Hz, CH_2), 5.21 (s, 2H, CH_2), 7.04–7.11 (m, 2H, Ar), 7.23–7.33 (m, 3H, Ar), 7.37–7.57 (m, 3H, Ar), 7.89–7.93 (m, 2H, Ar), 10.51 (s, 1H, NH); ^{13}C NMR ($CDCl_3$, 50 MHz, ppm): δ 22.2, 29.7, 49.8, 96.5, 120.4, 122.8, 126.4, 127.4, 128.7, 128.8, 132.0, 132.7, 136.8, 138.5, 140.9, 141.9, 145.3, 156.4, 164.4. Anal calcd for $C_{23}H_{17}Br_2N_3OS$: C, 50.85; H, 3.15; N, 7.73. Found: C, 50.69; H, 3.03; N, 7.85.

*5.1.5.3. N-[6,8-dibromo-7-(4-methoxybenzyl)-5,7-dihydro-4H-[1,3]thiazolo[4,5-e]isoindol-2-yl]benzamide (**12c**).* This compound was obtained from reaction of **11c** with benzoyl chloride. Yellow solid; yield 65%; mp 166–167 °C; IR cm^{-1}: 3496 (NH), 1641 (CO); ^1H NMR ($CDCl_3$, 200 MHz, ppm): δ 2.78 (t, 2H, *J*= 7.2 Hz, CH_2), 2.99 (t, 2H, *J*= 7.2 Hz, CH_2), 3.77 (s, 3H, CH_3), 5.15 (s, 2H, CH_2), 6.82 (d, 2H, *J*= 8.7 Hz, H-3' and H-5'), 7.05 (d, 2H, *J*= 8.7 Hz, H-2' and H-6'), 7.38–7.57 (m, 3H, H-3", H-4" and H-5"), 7.91 (d, 2H, *J*= 7.0 Hz, H-2" and H-6"), 10.47 (s, 1H, NH); ^{13}C NMR ($CDCl_3$, 50 MHz, ppm): δ 21.4, 22.7, 49.4, 55.3, 93.7, 96.2, 103.8, 108.0, 114.0, 120.4, 120.9, 122.8, 127.4, 127.9, 128.8, 130.6, 132.1, 132.8, 158.9, 164.4. Anal calcd for $C_{24}H_{19}Br_2N_3O_2S$: C, 50.28; H, 3.34; N, 7.33. Found: C, 50.15; H, 3.23; N, 7.51.

*5.1.5.4. N-[6-phenyl-7-(phenylsulfonyl)-5,7-dihydro-4H-[1,3]thiazolo[4,5-e]isoindol-2-yl]benzamide (**12d**).* This compound was obtained from reaction of **11d** with benzoyl chloride. White solid; yield 82%; mp 131–132 °C; IR cm^{-1}: 3148 (NH), 1668 (CO); ^1H NMR (DMSO-d_6, 200 MHz, ppm): δ 2.56 (t, 2H, *J*= 7.0 Hz, CH_2), 2.88 (t, 2H, *J*= 7.0 Hz, CH_2), 7.19–7.24 (m, 2H, Ar), 7.40–7.73 (m, 12H, Ar), 8.13 (d, 2H, *J*= 6.9 Hz, Ar), 12.73 (s, 1H, NH); ^{13}C NMR (DMSO-d_6, 50 MHz, ppm): δ 19.8, 21.3, 114.5, 121.2, 124.4, 124.6, 126.5, 127.6, 128.1, 128.4, 128.6, 129.5, 129.6, 130.8, 130.9, 131.8, 132.6, 134.4, 137.5, 138.8, 157.0, 164.8. Anal calcd for $C_{28}H_{21}N_3O_3S_2$: C, 65.73; H, 4.14; N, 8.21. Found: C, 65.64; H, 4.02; N, 8.45.

*5.1.5.5. N-(7-benzyl-8-bromo-6-phenyl-5,7-dihydro-4H-[1,3]thiazolo[4,5-e]isoindol-2-yl)benzamide (**12e**).* This compound was obtained from reaction of **11e** with benzoyl chloride. Yellow solid; yield 68%; mp 180–181 °C; IR cm^{-1}: 3405 (NH), 1666 (CO); ^1H NMR ($CDCl_3$, 200 MHz, ppm): δ 2.83 (t, 2H, *J*= 6.1 Hz, CH_2), 2.96 (t, 2H, *J*= 6.1 Hz, CH_2), 5.10 (s, 2H, CH_2), 6.85–6.90 (m, 2H, Ar), 7.17–7.22 (m, 5H, Ar), 7.30–7.56 (m, 6H, Ar), 7.89–7.93 (m, 2H, Ar), 10.64 (s, 1H, NH); ^{13}C NMR ($CDCl_3$, 50 MHz, ppm): δ 20.9, 22.8, 49.1, 98.4, 114.6, 118.2, 126.1,

127.2, 128.0, 128.1, 128.5, 128.6, 128.9, 129.9, 131.4, 132.0, 133.1, 137.8, 155.7, 155.8, 157.4, 157.6, 164.6. Anal calcd for $C_{29}H_{22}BrN_3OS$: C, 64.45; H, 4.10; N, 7.77. Found: C, 64.57; H, 3.98; N, 7.90.

*5.1.5.6. N-[8-bromo-7-(4-methoxybenzyl)-6-phenyl-5,7-dihydro-4H-[1,3]thiazolo[4,5-e]isoindol-2-yl]benzamide (**12f**).* This compound was obtained from reaction of **11f** with benzoyl chloride. Dark yellow solid; yield 72%; mp 175–176 °C; IR cm^{-1}: 3403 (NH), 1663 (CO); ^1H NMR ($CDCl_3$, 200 MHz, ppm): δ 2.82 (t, 2H, *J*= 6.6 Hz, CH_2), 2.96 (t, 2H, *J*= 6.6 Hz, CH_2), 3.75 (s, 3H, CH_3), 5.07 (s, 2H, CH_2), 6.74 (d, 2H, *J*= 8.9 Hz, H-3' and H-5'), 6.82 (d, 2H, *J*= 8.9 Hz, H-2' and H-6'), 7.18–7.23 (m, 2H, Ar), 7.32–7.59 (m, 6H, Ar), 7.95 (d, 2H, *J*= 6.9 Hz, Ar), 10.37 (s, 1H, NH); ^{13}C NMR ($CDCl_3$, 50 MHz, ppm): δ 21.1, 22.9, 48.4, 55.2, 97.8, 113.9, 116.5, 118.5, 122.5, 127.3, 127.5, 127.7, 128.5, 128.8, 129.9, 130.2, 131.6, 131.8, 132.2, 132.5, 140.4, 156.1, 158.6, 164.4. Anal calcd for $C_{30}H_{24}BrN_3O_2S$: C, 63.16; H, 4.24; N, 7.37. Found: C, 63.02; H, 4.19; N, 7.48.

*5.1.5.7. N-[7-(phenylsulfonyl)-6-(3,4,5-trimethoxyphenyl)-5,7-dihydro-4H-[1,3]thiazolo[4,5-e]isoindol-2-yl]benzamide (**12g**).* This compound was obtained from reaction of **11g** with benzoyl chloride. Light green solid; yield 79%; mp 211–212 °C; IR cm^{-1}: 3397 (NH), 1669 (CO); ^1H NMR (DMSO-d_6, 200 MHz, ppm): δ 2.61 (t, 2H, *J*= 6.9 Hz, CH_2), 2.91 (t, 2H, *J*= 6.9 Hz, CH_2), 3.71 (s, 6H, 2 x CH_3), 3.75 (s, 3H, CH_3), 6.42 (s, 2H, H-2" and H-6"), 7.43–7.70 (m, 9H, Ar), 8.13 (d, 2H, *J*= 6.9 Hz, Ar), 12.73 (s, 1H, NH); ^{13}C NMR (DMSO-d_6, 50 MHz, ppm): δ 19.8, 21.3, 55.9, 60.1, 108.6, 114.1, 114.2, 116.5, 120.6, 124.1, 124.7, 126.7, 128.1, 128.6, 129.4, 130.7, 131.9, 132.7, 134.3, 135.0, 137.6, 137.7, 152.0, 165.6. Anal calcd for $C_{31}H_{27}N_3O_6S_2$: C, 61.88; H, 4.52; N, 6.98. Found: C, 61.97; H, 4.43; N, 7.07.

*5.1.5.8. N-[7-benzyl-8-bromo-6-(3,4,5-trimethoxyphenyl)-5,7-dihydro-4H-[1,3]thiazolo[4,5-e]isoindol-2-yl]-4-methoxybenzamide (**12h**).* This compound was obtained from reaction of **11h** with benzoyl chloride. Dark brown solid; yield 60%; mp 177–178 °C; IR cm^{-1}: 3405 (NH), 1669 (CO); ^1H NMR (DMSO-d_6, 200 MHz, ppm): δ 2.81 (t, 2H, *J*= 6.4 Hz, CH_2), 2.94 (t, 2H, *J*= 6.4 Hz, CH_2), 3.58 (s, 6H, 2 x CH_3), 3.67 (s, 3H, CH_3), 5.20 (s, 2H, CH_2), 6.49 (s, 2H, H-2" and H-6"), 6.99 (d, 2H, *J*= 8.3 Hz, Ar), 7.20–7.37 (m, 3H, Ar), 7.49–7.67 (m, 3H, Ar), 8.11 (d, 2H, *J*= 8.3 Hz, Ar), 12.52 (s, 1H, NH); ^{13}C NMR (DMSO-d_6, 50 MHz, ppm): δ 20.7, 22.0, 48.7, 55.6, 60.0, 97.5, 106.9, 116.3, 118.0, 121.6, 125.6, 126.5, 126.9, 128.2, 128.4, 128.6, 131.3, 132.2, 132.4, 137.0, 138.5, 140.1, 152.7, 155.7, 165.0. Anal calcd for $C_{32}H_{28}BrN_3O_4S$: C, 60.95; H, 4.48; N, 6.66. Found: C, 61.09; H, 4.34; N, 6.77.

*5.1.5.9. N-[7-(4-methoxybenzyl)-8-bromo-6-(3,4,5-trimethoxyphenyl)-5,7-dihydro-4H-[1,3]thiazolo[4,5-e]isoindol-2-yl]-benzamide (**12i**).* This compound was obtained from reaction of **11i** with benzoyl chloride. Dark yellow solid; yield 64%; mp 118–119 °C; IR cm^{-1}: 3407 (NH),

1662 (CO); ^{1}H NMR (DMSO-*d*$_6$, 200 MHz, ppm): δ 2.80 (t, 2H, *J*= 6.0 Hz, CH_2), 2.93 (t, 2H, *J*= 6.0 Hz, CH_2), 3.64 (s, 6H, 2 x CH_3), 3.68 (s, 3H, CH_3), 3.70 (s, 3H, CH_3), 5.12 (s, 2H, CH_2), 6.53 (s, 2H, H-2" and H-6"), 6.82–6.99 (m, 4H, Ar), 7.51–7.67 (m, 3H, Ar), 8.12 (d, 2H, *J*= 7.0 Hz, Ar), 12.59 (d, 1H, NH); ^{13}C NMR (DMSO-*d*$_6$, 50 MHz, ppm): δ 20.6, 22.0, 48.1, 55.1, 55.7, 60.0, 97.4, 106.9, 113.9, 117.0, 121.4, 127.0, 128.2, 128.4, 129.5, 130.1, 131.2, 132.1, 132.4, 137.0, 139.8, 140.1, 152.8, 156.0, 158.3, 165.0. Anal calcd for $C_{33}H_{30}BrN_3O_5S$: C, 60.00; H, 4.58; N, 6.36. Found: C, 60.11; H, 4.43; N, 6.29.

*5.1.5.10. N-(7-benzyl-6,8-dibromo-5,7-dihydro-4H-[1,3]thiazolo[4,5-e]isoindol-2-yl)-4-methoxybenzamide (**12j**).* This compound was obtained from reaction of **11b** with 4-methoxybenzoyl chloride. White solid; yield 60%; mp 187–188 °C; IR cm^{-1}: 3535 (NH), 1645 (CO); ^{1}H NMR (DMSO-*d*$_6$, 200 MHz, ppm): δ 2.71 (t, 2H, *J*= 7.1 Hz, CH_2), 3.00 (t, 2H, *J*= 7.1 Hz, CH_2), 3.85 (s, 3H, CH_3), 5.27 (s, 2H, CH_2), 7.04–7.12 (m, 4H, Ar), 7.27–7.40 (m, 3H, Ar), 8.12 (d, 2H, *J*= 8.9 Hz, Ar), 12.36 (s, 1H, NH); ^{13}C NMR (DMSO-*d*$_6$, 50 MHz, ppm): δ 20.9, 21.4, 49.3, 55.5, 96.2, 100.1, 113.7, 117.7, 120.1, 121.9, 124.2, 126.0, 127.3, 128.7, 130.3, 137.0, 139.1, 156.2, 162.6, 164.4. Anal calcd for $C_{24}H_{19}Br_2N_3O_2S$: C, 50.28; H, 3.34; N, 7.33. Found: C, 50.11; H, 3.45; N, 7.21.

*5.1.5.11. N-[6,8-dibromo-7-(4-methoxybenzyl)-5,7-dihydro-4H-[1,3]thiazolo[4,5-e]isoindol-2-yl]-4-methoxybenzamide (**12k**).* This compound was obtained from reaction of **11c** with 4-methoxybenzoyl chloride. Light brown solid; yield 64%; mp 131–132 °C; IR cm^{-1}: 3404 (NH), 1646 (CO); ^{1}H NMR ($CDCl_3$, 200 MHz, ppm): δ 2.74–2.82 (m, 2H, CH_2), 2.93–3.01 (m, 2H, CH_2), 3.75 (s, 3H, CH_3), 3.80 (s, 3H, CH_3), 5.12 (s, 2H, CH_2), 6.80 (d, 2H, *J*= 8.8 Hz, Ar), 6.85 (d, 2H, *J*= 8.8 Hz, Ar), 7.05 (d, 2H, *J*= 8.8 Hz, Ar), 7.95 (d, 2H, *J*= 8.8 Hz, Ar), 10.52 (s, 1H, NH); ^{13}C NMR ($CDCl_3$, 50 MHz, ppm): δ 21.4, 22.2, 49.3, 55.3, 55.5, 91.2, 96.3, 113.9, 114.0, 120.4, 122.3, 124.2, 128.0, 128.8, 129.6, 134.6, 157.0, 158.9, 163.1, 163.8, 164.1. Anal calcd for $C_{25}H_{21}Br_2N_3O_3S$: C, 49.77; H, 3.51; N, 6.96. Found: C, 49.59; H, 3.38; N, 7.08.

*5.1.5.12. N-(7-benzyl-8-bromo-6-phenyl-5,7-dihydro-4H-[1,3]thiazolo[4,5-e]isoindol-2-yl)-4-methoxybenzamide (**12l**).* This compound was obtained from reaction of **11e** with 4-methoxybenzoyl chloride. Yellow solid; yield 70%; mp 169–170 °C; IR cm^{-1}: 3400 (NH), 1671 (CO); ^{1}H NMR ($CDCl_3$, 200 MHz, ppm): δ 2.83 (t, 2H, *J*= 6.5 Hz, CH_2), 2.95 (t, 2H, *J*= 6.5 Hz, CH_2), 3.85 (s, 3H, CH_3), 5.14 (s, 2H, CH_2), 6.89–6.96 (m, 4H, Ar), 7.19–7.24 (m, 5H, Ar), 7.33–7.36 (m, 3H, Ar), 7.96 (d, 2H, *J*= 8.7 Hz, Ar), 10.50 (s, 1H, NH); ^{13}C NMR ($CDCl_3$, 50 MHz, ppm): δ 20.8, 22.8, 49.0, 55.5, 98.5, 114.3, 118.1, 121.0, 123.3, 124.6, 126.1, 127.2, 128.0, 128.5, 128.6,

129.6, 129.9, 130.3, 131.3, 132.1, 137.7, 147.4, 163.6, 164.0. Anal calcd for $C_{30}H_{24}BrN_3O_2S$: C, 63.16; H, 4.24; N, 7.37. Found: C, 63.02; H, 4.44; N, 7.60.

*5.1.5.13. N-[8-bromo-7-(4-methoxybenzyl)-6-phenyl-5,7-dihydro-4H-[1,3]thiazolo[4,5-e]isoindol-2-yl]-4-methoxybenzamide (**12m**).* This compound was obtained from reaction of **11f** with 4-methoxybenzoyl chloride. Brown solid; yield 64%; mp 162–163 °C; IR cm^{-1}: 3408 (NH), 1655 (CO); ^{1}H NMR (DMSO-d_6, 200 MHz, ppm): δ 2.73 (t, 2H, *J*= 6.9 Hz, CH_2), 2.90 (t, 2H, *J*= 6.9 Hz, CH_2), 3.69 (s, 3H, CH_3), 3.85 (s, 3H, CH_3), 5.12 (s, 2H, CH_2), 6.76–6.86 (m, 4H, Ar), 7.06 (d, 2H, *J*= 8.9 Hz, Ar), 7.29–7.47 (m, 5H, Ar), 8.13 (d, 2H, *J*= 8.9 Hz, Ar), 12.34 (s, 1H, NH); ^{13}C NMR (DMSO-d_6, 50 MHz, ppm): δ 20.7, 22.0, 47.8, 55.0, 55.5, 113.7, 113.9, 116.6, 118.2, 121.4, 124.2, 126.9, 127.7, 128.5, 128.6, 129.5, 130.0, 130.3, 131.1, 131.2, 144.4, 155.9, 158.2, 162.5, 164.4. Anal calcd for $C_{31}H_{26}BrN_3O_3S$: C, 62.00; H, 4.36; N, 7.00. Found: C, 61.88; H, 4.19; N, 7.17.

*5.1.5.14. N-[7-benzyl-8-bromo-6-(3,4,5-trimethoxyphenyl)-5,7-dihydro-4H-[1,3]thiazolo[4,5-e]isoindol-2-yl]-4-methoxybenzamide (**12n**).* This compound was obtained from reaction of **11h** with 4-methoxybenzoyl chloride. Brown solid; yield 65%; mp 186–187 °C; IR cm^{-1}: 3152 (NH), 1657 (CO); ^{1}H NMR (DMSO-d_6, 200 MHz, ppm): δ 2.81–2.92 (m, 4H, 2 x CH_2), 3.58 (s, 6H, 2 x CH_3), 3.67 (s, 3H, CH_3), 3.86 (s, 3H, CH_3), 5.20 (s, 2H, CH_2), 6.49 (s, 2H, H-2" and H-6"), 6.98–7.09 (m, 4H, Ar), 7.24–7.38 (m, 3H, Ar), 8.14 (d, 2H, *J*= 8.4 Hz, Ar), 12.38 (s, 1H, NH); ^{13}C NMR (DMSO-d_6, 50 MHz, ppm): δ 20.7, 22.0, 48.6, 55.5, 55.6, 60.0, 106.8, 110.1, 113.7, 116.4, 118.0, 121.2, 121.4, 124.2, 125.5, 126.5, 126.9, 128.6, 130.3, 131.2, 136.9, 138.6, 152.7, 155.8, 162.5, 164.3. Anal calcd for $C_{33}H_{30}BrN_3O_5S$: C, 60.00; H, 4.58; N, 6.36. Found: C, 60.13; H, 4.65; N, 6.27.

*5.1.5.15. N-[8-bromo-7-(4-methoxybenzyl)-6-(3,4,5-trimethoxyphenyl)-5,7-dihydro-4H-[1,3]thiazolo[4,5-e]isoindol-2-yl]-4-methoxybenzamide (**12o**).* This compound was obtained from reaction of **11i** with 4-methoxybenzoyl chloride. Brown solid; yield 65%; mp 128–129 °C; IR cm^{-1}: 3404 (NH), 1662 (CO); ^{1}H NMR (DMSO-d_6, 200 MHz, ppm): δ 2.79 (t, 2H, *J*= 6.1 Hz, CH_2), 2.91 (t, 2H, *J*= 6.1 Hz, CH_2), 3.63 (s, 6H, 2 x CH_3), 3.68 (s, 3H, CH_3), 3.70 (s, 3H, CH_3), 3.85 (s, 3H, CH_3), 5.12 (s, 2H, CH_2), 6.52 (s, 2H, H-2" and H-6"), 6.81–6.94 (m, 4H, Ar), 7.07 (d, 2H, *J*= 8.7 Hz, Ar), 8.13 (d, 2H, *J*= 8.7 Hz, Ar), 12.38 (d, 1H, NH); ^{13}C NMR (DMSO-d_6, 50 MHz, ppm): δ 20.7, 22.0, 46.8, 55.1, 55.5, 55.7, 60.0, 97.3, 107.0, 113.7, 114.0, 117.0, 118.0, 121.2, 124.2, 126.4, 126.6, 127.0, 129.4, 130.3, 137.0, 152.7, 152.8, 156.2, 158.3, 162.5, 164.3. Anal calcd for $C_{34}H_{32}BrN_3O_6S$: C, 59.13; H, 4.67; N, 6.08. Found: C, 59.02; H, 4.87; N, 5.96.

*5.1.5.16. N-[6-phenyl-7-(phenylsulfonyl)-5,7-dihydro-4H-[1,3]thiazolo[4,5-e]isoindol-2-yl]acetamide (**12p**).* This compound was obtained from reaction of **11d** with acetyl chloride. White solid; yield 72%; mp 173–174 °C; IR cm^{-1}: 3396 (NH), 1653 (CO); ^{1}H NMR (DMSO-d_6, 200 MHz,

ppm): δ 2.15 (s, 3H, CH_3), 2.49–2.56 (m, 2H, CH_2), 2.83 (t, 2H, *J*= 7.3 Hz, CH_2), 7.16–7.21 (m, 2H, Ar), 7.37–7.55 (m, 8H, Ar), 7.64–7.72 (m, 1H, Ar), 12.19 (s, 1H, NH); ^{13}C NMR (DMSO-d_6, 50 MHz, ppm): δ 19.8, 21.2, 22.4, 114.4, 121.1, 123.6, 124.5, 126.5, 127.6, 128.4, 129.5, 129.7, 130.8, 130.9, 134.4, 137.6, 138.4, 156.5, 168.3. Anal calcd for $C_{23}H_{19}N_3O_3S_2$: C, 61.45; H, 4.26; N, 9.35. Found: C, 61.52; H, 4.13; N, 9.24.

*5.1.5.17. N-[8-bromo-7-(4-methoxybenzyl)-6-phenyl-5,7-dihydro-4H-[1,3]thiazolo[4,5-e]isoindol-2-yl]acetamide (**12q**).* This compound was obtained from reaction of **11f** with acetyl chloride. Light brown solid; yield 87%; mp 173–174 °C; IR cm^{-1}: 3409 (NH), 1700 (CO); ^{1}H NMR (DMSO-d_6, 200 MHz, ppm): δ 2.15 (s, 3H, CH_3), 2.71 (t, 2H, *J*= 6.6 Hz, CH_2), 2.85 (t, 2H, *J*= 6.6 Hz, CH_2), 3.69 (s, 3H, CH_3), 5.10 (s, 2H, CH_2), 6.76–6.86 (m, 4H, Ar), 7.28–7.43 (m, 5H, Ar), 12.08 (s, 1H, NH); ^{13}C NMR (DMSO-d_6, 50 MHz, ppm): δ 20.7, 22.0, 22.4, 47.8, 55.0, 97.4, 113.9, 116.5, 118.1, 120.8, 126.9, 127.7, 128.6, 129.5, 130.0, 131.1, 131.2, 139.6, 155.3, 158.2, 168.3. Anal calcd for $C_{25}H_{22}BrN_3O_2S$: C, 59.06; H, 4.36; N, 8.26. Found: C, 58.89; H, 4.52; N, 8.11.

*5.1.5.18. N-[7-(phenylsulfonyl)-6-(3,4,5-trimethoxyphenyl)-5,7-dihydro-4H-[1,3]thiazolo[4,5-e]isoindol-2-yl]acetamide (**12r**).* This compound was obtained from reaction of **11g** with acetyl chloride. White solid; yield 76%; mp 127–128 °C; IR cm^{-1}: 3448 (NH), 1664 (CO); ^{1}H NMR (DMSO-d_6, 200 MHz, ppm): δ 2.15 (s, 3H, CH_3), 2.57 (t, 2H, *J*= 7.0 Hz, CH_2), 2.85 (t, 2H, *J*= 7.0 Hz, CH_2), 3.69 (s, 6H, 2 x CH_3), 3.74 (s, 3H, CH_3), 6.39 (s, 2H, H-2" and H-6"), 7.38 (s, 1H, H-8), 7.42–7.57 (m, 4H, Ar), 7.69 (t, 1H, *J*= 7.0 Hz, Ar), 12.18 (s, 1H, NH); ^{13}C NMR (DMSO-d_6, 50 MHz, ppm): δ 19.8, 21.2, 22.4, 55.8, 60.1, 108.6, 114.1, 120.6, 123.4, 124.0, 124.7, 126.7, 129.4, 130.6, 134.3, 135.5, 137.7, 138.4, 152.0, 156.4, 168.3. Anal calcd for $C_{26}H_{25}N_3O_6S_2$: C, 57.87; H, 4.67; N, 7.79. Found: C, 57.69; H, 4.80; N, 7.92.

*5.1.5.19. N-[8-bromo-7-(4-methoxybenzyl)-6-(3,4,5-trimethoxyphenyl)-5,7-dihydro-4H-[1,3]thiazolo[4,5-e]isoindol-2-yl]acetamide (**12s**).* This compound was obtained from reaction of **11i** with acetyl chloride. Brown solid; yield 67%; mp 127–128 °C; IR cm^{-1}: 3378 (NH), 1680 (CO); ^{1}H NMR (DMSO-d_6, 200 MHz, ppm): δ 2.15 (s, 3H, CH_3), 2.73–2.87 (m, 4H, 2 x CH_2), 3.61 (s, 3H, CH_3), 3.67 (s, 3H, CH_3), 3.70 (s, 6H, 2 x CH_3), 5.10 (s, 2H, CH_2), 6.51 (s, 2H, H-2" and H-6"), 6.81–6.89 (m, 4H, Ar), 12.12 (d, 1H, NH); ^{13}C NMR (DMSO-d_6, 50 MHz, ppm): δ 20.8, 22.0, 22.4, 47.9, 55.1, 55.7, 60.0, 96.9, 106.9, 109.9, 113.3, 114.0, 116.9, 126.9, 129.4, 130.3, 137.0, 139.3, 152.7, 155.2, 155.6, 158.2, 168.3. Anal calcd for $C_{28}H_{28}BrN_3O_5S$: C, 56.19; H, 4.72; N, 7.02. Found: C, 56.01; H, 4.88; N, 6.95.

4.2. Biology

4.2.1. Flow cytometric analysis of cell cycle distribution

HeLa cells were treated with different concentrations of the test compounds for 24 h. After the incubation period, the cells were collected, centrifuged, and fixed with ice-cold ethanol (70%). The cells were then treated with lysis buffer containing RNase A and 0.1% Triton X-100 and stained with PI. Samples were analyzed on a Cytomic FC500 flow cytometer (Beckman Coulter). DNA histograms were analyzed using MultiCycle for Windows (Phoenix Flow Systems).

4.2.2. Apoptosis assay

Cell death was determined by flow cytometry of cells double stained with annexin V/FITC and PI. The Coulter Cytomics FC500 (Beckman Coulter) was used to measure the surface exposure of phosphatidyl serine on apoptotic cells according to the manufacturer's instructions (Annexin-V Fluos, Roche Diagnostics).

4.2.3. Assessment of mitochondrial potential

The mitochondrial membrane potential was measured with the lipophilic cationic dye 5,5′,6,6′ tetrachloro-1,1′,3,3′-tetraethylbenzimidazol-carbocyanine (JC-1) (Molecular Probes), as described [54]. The method is based on the ability of this fluorescent probe to enter selectively into the mitochondria since its color changes reversibly from green to red as membrane potential increases. This property is due to the reversible formation of JC-1 aggregates upon membrane polarization that causes a shift in the emitted light from 530 nm (i.e., emission of JC-1 monomeric form) to 590 nm (emission of JC-1 aggregate) when excited at 490 nm. Consequently, the cells analyzed at 530 nm correspond to cells with a low $\Delta\Psi_{mt}$.

4.2.4. Western blot analysis

HeLa cells were incubated in the presence of the test compound and, after different times, were collected, centrifuged, and washed two times with ice cold phosphate buffered saline (PBS). The pellet was then resuspended in lysis buffer. After the cells were lysed on ice for 30 min, lysates were centrifuged at 15000 x g at 4 °C for 10 min. The protein concentration in the supernatant was determined using the BCA protein assay reagents (Pierce, Italy). Equal amounts of protein (10 μg) were resolved using sodium dodecyl sulfate-polyacrylamide gel electrophoresis (Criterion Precast, BioRad, Italy) and transferred to a PVDF Hybond-P membrane (GE Healthcare). Membranes were blocked with a bovine serum albumin solution (5% in Tween PBS 1X), the membranes being gently rotated overnight at 4 °C. Membranes were then incubated with primary antibodies against caspase-9 cleaved fragment, PARP, cdc25c, cyclin B, p-cdc2^{Y15} (all from Cell Signaling), or vinculin (Sigma-

Aldrich) for 2 h at room temperature. Membranes were next incubated with peroxidase labeled secondary antibodies for 1 h. All membranes were visualized using ECL Select (GE Healthcare), and images were acquired using a Uvitec-Alliance imaging system (Uvitec, Cambridge, UK). To ensure equal protein loading, each membrane was stripped and reprobed with an anti-vinculin antibody.

4.2.5. Statistical analysis

The differences between different treatments were analyzed, using the two-sided Student's t test. P values lower than 0.05 were considered significant.

4.2.6. Tubulin studies

4.2.6.1. Inhibition of tubulin assembly

Electrophoretically homogeneous bovine brain tubulin was prepared as previously described [55]. Tubulin assembly was measured turbidimetrically at 350 nm in Beckman recording spectrophotometers with electronic temperature controllers by methods described previously [56]. However, the tubulin used in the experiments described here was more active than that used previously. Therefore, the concentration of tubulin was reduced from 10 to 9 μM (1.0 to 0.9 mg/mL) and that of GTP from 0.4 to 0.2 mM. This allowed us to reproduce the earlier IC_{50} value obtained for the standard agent CA-4.

4.2.6.2. Inhibition of binding of [^{3}H]colchicine to tubulin

Identical reaction conditions were used as previously described [57], except that the tubulin concentration was reduced from 0.1 mg/mL to 0.05 mg/mL (0.05 μM) and one, rather than two, DEAE-cellulose filters was used for each reaction mixture.

4.3. Molecular modeling

4.3.1. Docking studies

The Schrödinger Suite version 2018 [58] was used to carry out all molecular modeling simulations for compounds **11c**, **11i** and **12s**, since they showed the best inhibitory activity in tubulin binding assays. Ligand structures were built with the graphical interface of Maestro and modeled by means of the LigPrep tool [59]. Their possible ionization states at pH 7.4 were generated by using OPLS_2005, as force field [60].

The tubulin structure with PDB code 4O2B [61] was selected as the colchicine-bound co-crystal structure and downloaded from the Protein Data Bank (PDB) [62]. Then, it was pre-processed using

the Schrödinger Protein Preparation Wizard by assigning bond orders, adding hydrogens and performing a restrained energy minimization of the added hydrogens using the OPLS_2005 force field. Moreover, all water molecules were removed, and the nucleotides (GTP and GDP) and metals (Mg^{2+} and Zn^{2+}) were retained.

The rigid receptor grid, defined by a 15×15×15 Å inner box, was generated by using as centroid the co-crystallized colchicine. Docking studies were performed by means of the software Glide *ver.* 7.8 [63]. With respect of the re-docking analysis, the Glide Standard-Precision (SP) protocol and the C and D chains of the PDB model were selected to perform the later computational studies (for details, see Supplementary Materials Paragraph "Redocking Analysis" and Table S1). For each ligand, we generated ten poses, by selecting the best binding mode through the evaluation of the default docking scoring function.

5.3.2. Molecular dynamics simulation studies (MDSs)

The stability over time of the best binding poses for compounds **11c**, **11i** and **12s** was further evaluated by MDS and compared with the colchicine complex. MD suitable systems were generated by means of the Desmond package [64]. Specifically, each complex was solvated in an orthorhombic box with a buffer of 10 Å TIP3P [65] (Transferable Intermolecular Potential 3-Point) water and neutralized by adding K^+ counter ions. The system was minimized and pre-equilibrated by means of the default relaxation routine implemented in Desmond. Simulation time was set to 20 ns, and the following conditions were applied: NPT ensemble, a temperature of 300K, a pressure of 1 bar, the Berendsen thermostat-barostat, and a recording interval equal to 40 ps both for energy and for trajectory. The time step was set to 2 fs. The Simulation Event Analysis tool of Desmond was used for MDS analyses, while visualization of protein-ligand complex was carried out using Maestro. Moreover, the Desmond Trajectory Clustering tool was used to generate the best representative structure of the whole MDS with the aim to describe induced-fit binding events of our compounds. Finally, these selected structures were submitted to the calculation of the ΔG_{bind} value by means the MM/GBSA method as implemented in the Prime module [66] from Maestro using the default settings.

Acknowledgements

This work was financially supported by Ministero dell'Istruzione dell'Università e della Ricerca (MIUR).

This research was supported in part by the Developmental Therapeutics Program in the Division of Cancer Treatment and Diagnosis of the National Cancer Institute, which includes federal funds under Contract No. HHSN261200800001E. The content of this publication does not necessarily reflect the views or policies of the Department of Health and Human Services, nor does mention of trade names, commercial products, or organizations imply endorsement by the U.S. Government.

The authors also thank the Developmental Therapeutic Program of the National Cancer Institute for performing cytotoxicity studies with selected compounds in the 60 cancer cell line screen.

The authors acknowledge the Italian Association for Cancer Research (AIRC) research project "Small molecule-based targeting of lncRNAs 3D structure: a translational platform for the treatment of multiple myeloma" (code 21588) and the PRIN 2017 research project "Novel anticancer agents endowed with multi-targeting mechanism of action" (code 201744BN5T)

References

[1] P.C. Diao, Q. Li, M.J. Hu, Y.F. Ma, W.W. You, K.H. Hong, P.L. Zhao, Synthesis and biological evaluation of novel indole-pyrimidine hybrids bearing morpholine and thiomorpholine moieties, Eur. J. Med. Chem. 134 (2017) 110–118. doi:10.1016/j.ejmech.2017.04.011.

[2] M.A. Jordan, L. Wilson, Microtubules as a target for anticancer drugs, Nat. Rev. Cancer. 4 (2004) 253–265. doi:10.1038/nr1317.

[3] M.B. Gordon, L. Howard, D.A. Compton, Chromosome movement in mitosis requires microtubule anchorage at spindle poles, J. Cell Biol. 153 (2001) 425–434. doi:10.1083/jcb.152.3.425.

[4] C. Dumontet, M.A. Jordan, Microtubule-binding agents: A dynamic field of cancer therapeutics, Nat. Rev. Drug Discov. 9 (2010) 790–803. doi:10.1038/nrd3253.

[5] V. Chaudhary, J.B. Venghateri, H.P.S. Dhaked, A.S. Bhoyar, S.K. Guchhait, D. Panda, Novel combretastatin-2-aminoimidazole analogues as potent tubulin assembly inhibitors: exploration of unique pharmacophoric impact of bridging skeleton and aryl moiety, J. Med.

Chem. 59 (2016) 3439–3451. doi:10.1021/acs.jmedchem.6b00101.

[6] A.V. Subba Rao, K. Swapna, S.P. Shaik, V. Lakshma Nayak, T. Srinivasa Reddy, S. Sunkari, T.B. Shaik, C. Bagul, A. Kamal, Synthesis and biological evaluation of *cis*-restricted triazole/tetrazole mimics of combretastatin-benzothiazole hybrids as tubulin polymerization inhibitors and apoptosis inducers, Bioorg. Med. Chem. 25 (2017) 977–999. doi:10.1016/j.bmc.2016.12.010.

[7] C.M. Lin, S.B. Singh, P.S. Chu, R.O. Dempcy, J.M. Schmidt, G.R. Pettit, E. Hamel, Interactions of tubulin with potent natural and synthetic analogs of the antimitotic agent combretastatin: A structure-activity study, Mol. Pharmacol. 34 (1988) 200–208.

[8] W. Li, F. Xu, W. Shuai, H. Sun, H. Yao, C. Ma, S. Xu, H. Yao, Z. Zhu, D.H. Yang, Z.S. Chen, J. Xu, Discovery of novel quinoline-chalcone derivatives as potent antitumor agents with microtubule polymerization inhibitory activity, J. Med. Chem. 62 (2019) 993–1013. doi:10.1021/acs.jmedchem.8b01755.

[9] T.F. Greene, S. Wang, L.M. Greene, S.M. Nathwani, J.K. Pollock, A.M. Malebari, T. McCabe, B. Twamley, N.M. O'Boyle, D.M. Zisterer, M.J. Meegan, Synthesis and biochemical evaluation of 3-phenoxy-1,4-diarylazetidin-2-ones as tubulin-targeting antitumor agents, J. Med. Chem. 59 (2016) 90–113. doi:10.1021/acs.jmedchem.5b01086.

[10] Y.L. Zhang, B.Y. Li, R. Yang, L.Y. Xia, A.L. Fan, Y.C. Chu, L.J. Wang, Z.C. Wang, A.Q. Jiang, H.L. Zhu, A class of novel tubulin polymerization inhibitors exert effective anti-tumor activity via mitotic catastrophe, Eur. J. Med. Chem. 163 (2019) 896–910. doi:10.1016/j.ejmech.2018.12.030.

[11] R. Romagnoli, P.G. Baraldi, A. Brancale, A. Ricci, E. Hamel, R. Bortolozzi, G. Basso, G. Viola, Convergent synthesis and biological evaluation of 2-amino-4-(3′,4′,5′-trimethoxyphenyl)-5-aryl thiazoles as microtubule targeting agents, J. Med. Chem. 54 (2011) 5144–5153. doi:10.1021/jm200392p.

[12] F. Wang, Z. Yang, Y. Liu, L. Ma, Y. Wu, L. He, M. Shao, K. Yu, W. Wu, Y. Pu, C. Nie, L. Chen, Synthesis and biological evaluation of diarylthiazole derivatives as antimitotic and antivascular agents with potent antitumor activity, Bioorg. Med. Chem. 23 (2015) 3337–3350. doi:10.1016/j.bmc.2015.04.055.

[13] Y. Lu, C.M. Li, Z. Wang, C.R. Ross, J. Chen, J.T. Dalton, W. Li, D.D. Miller, Discovery of

4-substituted methoxybenzoyl-aryl-thiazoles as novel anticancer agents: Synthesis, biological evaluation, and structure-activity relationships, J. Med. Chem. 52 (2009) 1701–1711. doi:10.1021/jm801449a.

[14] C.M. Li, Z. Wang, Y. Lu, S. Ahn, R. Narayanan, J.D. Kearbey, D.N. Parke, W. Li, D.D. Miller, J.T. Dalton, Biological activity of 4-substituted methoxybenzoyl-aryl-thiazole: An active microtubule inhibitor, Cancer Res. 71 (2011) 216–224. doi:10.1158/0008-5472.CAN-10-1725.

[15] Y. Lu, C.M. Li, Z. Wang, J. Chen, M.L. Mohler, W. Li, J.T. Dalton, D.D. Miller, Design, synthesis, and SAR studies of 4-substituted methoxylbenzoyl-aryl-thiazole analogues as potent and orally bioavailable anticancer agents, J. Med. Chem. 54 (2011) 4678–4693. doi:10.1021/jm2003427.

[16] P.C. Diao, W.Y. Lin, X.E. Jian, Y.H. Li, W.W. You, P.L. Zhao, Discovery of novel pyrimidine-based benzothiazole derivatives as potent cyclin-dependent kinase 2 inhibitors with anticancer activity, Eur. J. Med. Chem. 179 (2019) 196–207. doi:10.1016/j.ejmech.2019.06.055.

[17] M. Okaniwa, M. Hirose, T. Arita, M. Yabuki, A. Nakamura, T. Takagi, T. Kawamoto, N. Uchiyama, A. Sumita, S. Tsutsumi, T. Tottori, Y. Inui, B.C. Sang, J. Yano, K. Aertgeerts, S. Yoshida, T. Ishikawa, Discovery of a selective kinase inhibitor (TAK-632) targeting pan-RAF inhibition: Design, synthesis, and biological evaluation of C-7-substituted 1,3-benzothiazole derivatives, J. Med. Chem. 56 (2013) 6478–6494. doi:10.1021/jm400778d.

[18] M. Gjorgjieva, T. Tomašič, M. Barančokova, S. Katsamakas, J. Ilaš, P. Tammela, L.P. Mašič, D. Kikelj, Discovery of benzothiazole scaffold-based DNA gyrase B inhibitors, J. Med. Chem. 59 (2016) 8941–8954. doi:10.1021/acs.jmedchem.6b00864.

[19] J. Ma, G. Bao, L. Wang, W. Li, B. Xu, B. Du, J. Lv, X. Zhai, P. Gong, Design, synthesis, biological evaluation and preliminary mechanism study of novel benzothiazole derivatives bearing indole-based moiety as potent antitumor agents, Eur. J. Med. Chem. 96 (2015) 173–186. doi:10.1016/j.ejmech.2015.04.018.

[20] L. Van Der Veen, D. McConnel, S. Schneider, M. Grauert, A. Schoop, T. Wunberg, Thia-triaza-as-indacenes as PI3-kinase inhibitors for the treatment of cancer, WO2010122091Al, 2010.

[21] S. Bhat, J.S. Shim, J.O. Liu, Tricyclic thiazoles are a new class of angiogenesis inhibitors, Bioorg. Med. Chem. Lett. 23 (2013) 2733–2737. doi:10.1016/j.bmcl.2013.02.067.

[22] S.P. Hong, K.G. Liu, G. Ma, M. Sabio, M.A. Uberti, M.D. Bacolod, J. Peterson, Z.Z. Zou, A.J. Robichaud, D. Doller, Tricyclic thiazolopyrazole derivatives as metabotropic glutamate receptor 4 positive allosteric modulators, J. Med. Chem. 54 (2011) 5070–5081. doi:10.1021/jm200290z.

[23] B. Parrino, A. Attanzio, V. Spanò, S. Cascioferro, A. Montalbano, P. Barraja, L. Tesoriere, P. Diana, G. Cirrincione, A. Carbone, Synthesis, antitumor activity and CDK1 inhibiton of new thiazole nortopsentin analogues, Eur. J. Med. Chem. 138 (2017) 371–383. doi:10.1016/j.ejmech.2017.06.052.

[24] J.L. Whatmore, E. Swann, P. Barraja, J.J. Newsome, M. Bunderson, H.D. Beall, J.E. Tooke, C.J. Moody, Comparative study of isoflavone, quinoxaline and oxindole families of anti-angiogenic agents, Angiogenesis 5 (2002) 45–51. doi:10.1023/A:1021528628524.

[25] P. Diana, A. Stagno, P. Barraja, A. Carbone, B. Parrino, F. Dall'Acqua, D. Vedaldi, A. Salvador, P. Brun, I. Castagliuolo, O.G. Issinger, G. Cirrincione, Synthesis of triazenoazaindoles: A new class of triazenes with antitumor activity, ChemMedChem 6 (2011) 1291–1299. doi:10.1002/cmdc.201100027.

[26] P. Barraja, L. Caracausi, P. Diana, A. Carbone, A. Montalbano, G. Cirrincione, P. Brun, G. Palù, I. Castagliuolo, F. Dall'Acqua, D. Vedaldi, A. Salvador, Synthesis of pyrrolo[3,2-*h*]quinolinones with good photochemotherapeutic activity and no DNA damage, Bioorg. Med. Chem. 18 (2010) 4830–4843. doi:10.1016/j.bmc.2010.04.080.

[27] P. Barraja, P. Diana, A. Lauria, A. Montalbano, A.M. Almerico, G. Dattolo, G. Cirrincione, G. Viola, F. Dall'Acqua, Pyrrolo[2,3-*h*]quinolinones: Synthesis and photochemotherapic activity, Bioorg. Med. Chem. Lett. 13 (2003) 2809–2811. doi:10.1016/S0960-894X(03)00529-8.

[28] P. Diana, P. Barraja, A. Lauria, A. Montalbano, A.M. Almerico, G. Dattolo, G. Cirrincione, Pyrrolo[2,1-*d*][1,2,3,5]tetrazine-4(3*H*)-ones, a new class of azolotetrazines with potent antitumor activity, Bioorg. Med. Chem. 11 (2003) 2371–2380. doi:10.1016/S0968-0896(03)00145-7.

[29] A. Lauria, M. Bruno, P. Diana, P. Barraja, A. Montalbano, G. Cirrincione, G. Dattolo, A.M.

Almerico, Annelated pyrrolo-pyrimidines from amino-cyanopyrroles and BMMAs as leads for new DNA-interactive ring systems, Bioorg. Med. Chem. 13 (2005) 1545–1553. doi:10.1016/j.bmc.2004.12.027.

[30] V. Spanò, A. Attanzio, S. Cascioferro, A. Carbone, A. Montalbano, P. Barraja, L. Tesoriere, G. Cirrincione, P. Diana, B. Parrino, Synthesis and antitumor activity of new thiazole nortopsentin analogs, Mar. Drugs 14 (2016). doi:10.3390/md14120226.

[31] B. Parrino, C. Ciancimino, A. Carbone, V. Spanò, A. Montalbano, P. Barraja, G. Cirrincione, P. Diana, Synthesis of isoindolo[1,4]benzoxazinone and isoindolo[1,5]benzoxazepine: Two new ring systems of pharmaceutical interest, Tetrahedron 71 (2015) 7332–7338. doi:10.1016/j.tet.2015.04.083.

[32] P. Barraja, V. Spanò, D. Giallombardo, P. Diana, A. Montalbano, A. Carbone, B. Parrino, G. Cirrincione, Synthesis of [1,2]oxazolo[5,4-*e*]indazoles as antitumour agents, Tetrahedron 69 (2013) 6474–6477. doi:10.1016/j.tet.2013.05.083.

[33] V. Spanò, A. Montalbano, A. Carbone, B. Parrino, P. Diana, G. Cirrincione, P. Barraja, Convenient synthesis of pyrrolo[3,4-*g*]indazole, Tetrahedron 69 (2013) 9839–9847. doi:10.1016/j.tet.2013.09.003.

[34] P. Barraja, P. Diana, V. Spanò, A. Montalbano, A. Carbone, B. Parrino, G. Cirrincione, An efficient synthesis of pyrrolo[3′,2′:4,5]thiopyrano[3,2-*b*]pyridin-2-one: A new ring system of pharmaceutical interest, Tetrahedron 68 (2012) 5087–5094. doi:10.1016/j.tet.2012.04.041.

[35] P. Diana, A. Stagno, P. Barraja, A. Montalbano, A. Carbone, B. Parrino, G. Cirrincione, Synthesis of the new ring system pyrrolizino[2,3-*b*]indol-4(5*H*)-one, Tetrahedron 67 (2011) 3374–3379. doi:10.1016/j.tet.2011.03.060.

[36] V. Spanò, M. Pennati, B. Parrino, A. Carbone, A. Montalbano, V. Cilibrasi, V. Zuco, A. Lopergolo, D. Cominetti, P. Diana, G. Cirrincione, P. Barraja, N. Zaffaroni, Preclinical activity of new [1,2]oxazolo[5,4-*e*]isoindole derivatives in diffuse malignant peritoneal mesothelioma, J. Med. Chem. 59 (2016) 7223–7238. doi:10.1021/acs.jmedchem.6b00777.

[37] V. Spanò, M. Pennati, B. Parrino, A. Carbone, A. Montalbano, A. Lopergolo, V. Zuco, D. Cominetti, P. Diana, G. Cirrincione, N. Zaffaroni, P. Barraja, [1,2]Oxazolo[5,4-*e*]isoindoles as promising tubulin polymerization inhibitors, Eur. J. Med. Chem. 124 (2016) 840–851. doi:10.1016/j.ejmech.2016.09.013.

[38] P. Barraja, L. Caracausi, P. Diana, V. Spanò, A. Montalbano, A. Carbone, B. Parrino, G. Cirrincione, Synthesis and antiproliferative activity of the ring system [1,2]oxazolo[4,5-*g*]indole, ChemMedChem 7 (2012) 1901–1904. doi:10.1002/cmdc.201200296.

[39] V. Spanò, R. Rocca, M. Barreca, D. Giallombardo, A. Montalbano, A. Carbone, M.V. Raimondi, E. Gaudio, R. Bortolozzi, R. Bai, P. Tassone, S. Alcaro, E. Hamel, G. Viola, F. Bertoni, P. Barraja, Pyrrolo[2',3':3,4]cycloepta[1,2-*d*][1,2]oxazoles, a new class of antimitotic agents, active against multiple malignant cell types, J. Med. Chem. 59 (2020) 12023–12042. doi:10.1021/acs.jmedchem.0c01315.

[40] V. Spanò, A. Montalbano, A. Carbone, B. Parrino, P. Diana, G. Cirrincione, I. Castagliuolo, P. Brun, O.G. Issinger, S. Tisi, I. Primac, D. Vedaldi, A. Salvador, P. Barraja, Synthesis of a new class of pyrrolo[3,4-*h*]quinazolines with antimitotic activity, Eur. J. Med. Chem. 74 (2014) 340–357. doi:10.1016/j.ejmech.2013.10.014.

[41] P. Barraja, V. Spanò, P. Diana, A. Carbone, G. Cirrincione, D. Vedaldi, A. Salvador, G. Viola, F. Dall'Acqua, Pyrano[2,3-*e*]isoindol-2-ones, new angelicin heteroanalogues, Bioorg. Med. Chem. Lett. 19 (2009) 1711–1714. doi:10.1016/j.bmcl.2009.01.096.

[42] P. Barraja, V. Spanò, P. Diana, A. Carbone, G. Cirrincione, Synthesis of the new ring system 6,8-dihydro-5*H*-pyrrolo[3,4-*h*]quinazoline, Tetrahedron Lett. 50 (2009) 5389–5391. doi:10.1016/j.tetlet.2009.07.045.

[43] A. Musacchio, The molecular biology of spindle assembly checkpoint signaling dynamics, Curr. Biol. 25 (2015) R1002–R1018. doi:10.1016/j.cub.2015.08.051.

[44] H.Y. Yamada, G.J. Gorbsky, Spindle checkpoint function and cellular sensitivity to antimitotic drugs, Mol. Cancer Ther. 5 (2006) 2963–2969. doi:10.1158/1535-7163.MCT-06-0319.

[45] H.J. Choi, M. Fukui, B.T. Zhu, Role of cyclin B1/cdc2 up-regulation in the development of mitotic prometaphase arrest in human breast cancer cells treated with nocodazole, PLoS One. 6 (2011). doi:10.1371/journal.pone.0024312.

[46] J.D. Ly, D.R. Grubb, A. Lawen, The mitochondrial membrane potential (δψm) in apoptosis; an update, Apoptosis 8 (2003) 115–128. doi:10.1023/A:1022945107762.

[47] D.R. Green, G. Kroemer, The pathophysiology of mitochondrial cell death, Science 305 (2004) 626–629. doi:10.1126/science.1099320.

[48] A. Rovini, A. Savry, D. Braguer, M. Carré, Microtubule-targeted agents: When mitochondria become essential to chemotherapy, Biochim. Biophys. Acta - Bioenerg. 1807 (2011) 679–688. doi:10.1016/j.bbabio.2011.01.001.

[49] R. Romagnoli, P.G. Baraldi, M.K. Salvador, D. Preti, M. Aghazadeh Tabrizi, A. Brancale, X.H. Fu, J. Li, S.Z. Zhang, E. Hamel, R. Bortolozzi, E. Porcù, G. Basso, G. Viola, Discovery and optimization of a series of 2-aryl-4-amino-5-(3′,4′,5′-trimethoxybenzoyl)thiazoles as novel anticancer agents, J. Med. Chem. 55 (2012) 5433–5445. doi:10.1021/jm300388h.

[50] R. Romagnoli, P.G. Baraldi, C. Lopez-Cara, M.K. Salvador, D. Preti, M.A. Tabrizi, J. Balzarini, P. Nussbaumer, M. Bassetto, A. Brancale, X.H. Fu, Y. Gao, J. Li, S.Z. Zhang, E. Hamel, R. Bortolozzi, G. Basso, G. Viola, Design, synthesis and biological evaluation of 3,5-disubstituted 2-amino thiophene derivatives as a novel class of antitumor agents, Bioorg. Med. Chem. 22 (2015) 5097–5109. doi:10.1016/j.bmc.2013.12.030.

[51] R. Romagnoli, P.G. Baraldi, M.K. Salvador, F. Prencipe, V. Bertolasi, M. Cancellieri, A. Brancale, E. Hamel, I. Castagliuolo, F. Consolaro, E. Porcù, G. Basso, G. Viola, Synthesis, antimitotic and antivascular activity of 1-(3′,4′,5′-trimethoxybenzoyl)-3-arylamino-5-amino-1,2,4-triazoles, J. Med. Chem. 57 (2014) 6795–6808. doi:10.1021/jm5008193.

[52] P. Li, L. Zhou, T. Zhao, X. Liu, P. Zhang, Y. Liu, X. Zheng, Q. Li, Caspase-9: Structure, mechanisms and clinical application, Oncotarget 8 (2017) 23996–24008. doi:10.18632/oncotarget.15098.

[53] C. Soldani, A.I. Scovassi, Poly(ADP-ribose) polymerase-1 cleavage during apoptosis : An update. Cell death mechanisms: Necrosis and apoptosis, Apoptosis 7 (2002) 321–328.

[54] S. Salvioli, A. Ardizzoni, C. Franceschi, A. Cossarizza, JC-1, but not DiOC6(3) or rhodamine 123, is a reliable fluorescent probe to assess ΔΨ changes in intact cells: Implications for studies on mitochondrial functionality during apoptosis, FEBS Lett. 411 (1997) 77–82. doi:10.1016/S0014-5793(97)00669-8.

[55] E. Hamel, C.M. Lin, Separation of active tubulin and microtubule-associated proteins by ultracentrifugation and isolation of a component causing the formation of microtubule bundles, Biochemistry. 23 (1984) 4173–4184. doi:10.1021/bi00313a026.

[56] E. Hamel, Evaluation of antimitotic agents by quantitative comparisons of their effects on the polymerization of purified tubulin, Cell Biochem. Biophys. 38 (2003) 1–21.

doi:10.1385/CBB:38:1:1.

[57] P. Verdier-Pinard, J.Y. Lai, H.D. Yoo, J. Yu, B. Marquez, D.G. Nagle, M. Nambu, J.D. White, J.R. Falck, W.H. Gerwick, B.W. Day, E. Hamel, Structure-activity analysis of the interaction of curacin A, the potent colchicine site antimitotic agent, with tubulin and effects of analogs on the growth of MCF-7 breast cancer cells, Mol. Pharmacol. 53 (1998) 62–76. doi:10.1124/mol.53.1.62.

[58] Schrödinger LLC, New York (USA), (2018).

[59] LigPrep; Maestro; Schrödinger Suites; Schrödinger, LLC: New York, NY, USA, (2018).

[60] D. Shivakumar, E. Harder, W. Damm, R.A. Friesner, W. Sherman, Improving the prediction of absolute solvation free energies using the next generation OPLS force field, J. Chem. Theory Comput. 8 (2012) 2553–2558. doi:10.1021/ct300203w.

[61] A.E. Prota, F. Danel, F. Bachmann, K. Bargsten, R.M. Buey, J. Pohlmann, S. Reinelt, H. Lane, M.O. Steinmetz, The novel microtubule-destabilizing drug BAL27862 binds to the colchicine site of tubulin with distinct effects on microtubule organization, J. Mol. Biol. 426 (2014) 1848–1860. doi:10.1016/j.jmb.2014.02.005.

[62] http://www.rcsb.org/, (2020).

[63] Glide, Schrödinger, LLC, New York, NY, (2018).

[64] K.J. Bowers, D.E. Chow, H. Xu, R.O. Dror, M.P. Eastwood, B.A. Gregersen, J.L. Klepeis, I. Kolossvary, M.A. Moraes, F.D. Sacerdoti, J.K. Salmon, Y. Shan, D.E. Shaw, Scalable algorithms for molecular dynamics simulations on commodity clusters, in: Proc. 2006 ACM/IEEE SC|06 Conf. (SC'06), (Tampa, FL), IEEE, 2006: pp. 43. doi:10.1109/sc.2006.54.

[65] Y. Tsujimoto, S. Shimizu, Role of the mitochondrial membrane permeability transition in cell death, Apoptosis 12 (2007) 835–840. doi:10.1007/s10495-006-0525-7.

[66] Prime, Schrödinger LLC, New York, NY, (2018).